

CAPITAL UNIVERSITY OF SCIENCE AND
TECHNOLOGY, ISLAMABAD



**Heat and Mass Transfer Analysis
of the Flow of a Williamson
Nanofluid using Buongiorno
Model**

by

Sajjad Hussain

A thesis submitted in partial fulfillment for the
degree of Master of Philosophy

in the

Faculty of Computing

Department of Mathematics

2021

Copyright © 2021 by Sajjad Hussain

All rights reserved. No part of this thesis may be reproduced, distributed, or transmitted in any form or by any means, including photocopying, recording, or other electronic or mechanical methods, by any information storage and retrieval system without the prior written permission of the author.

I dedicate my dissertation work to my grandmother (late).

A special feeling of gratitude to,

My Father Mr. Yahya Khan, My Mother Noor Jahan,

My Grandfather and All Family.

*A determined and aristocratic embodiment who educate me to belief in **ALLAH**,
who have supported me financially and encouraged me in my difficult time and
without constant compelling to make me study I would never have been achieved
this milestone.*



CERTIFICATE OF APPROVAL

Heat and Mass Transfer Analysis of the Flow of a Williamson Nanofluid using Buongiorno Model

by

Sajjad Hussain

(MMT191007)

THESIS EXAMINING COMMITTEE

- | | | | |
|-----|-------------------|----------------------|-----------------|
| (a) | External Examiner | Dr. Shagufta Ijaz | HITECH, Taxila |
| (b) | Internal Examiner | Dr. Samina Rashid | CUST, Islamabad |
| (c) | Supervisor | Dr. Muhammad Sagheer | CUST, Islamabad |

Dr. Muhammad Sagheer

Thesis Supervisor

December, 2021

Dr. Muhammad Sagheer

Head

Dept. of Mathematics

December, 2021

Dr. Muhammad Abdul Qadir

Dean

Faculty of Computing

December, 2021

Author's Declaration

I, **Sajjad Hussain**, hereby state that my M.Phil thesis titled “**Heat and Mass Transfer Analysis of the Flow of a Williamson Nanofluid using Buongiorno Model**” is my own work and has not been submitted previously by me for taking any degree from Capital University of Science and Technology, Islamabad or anywhere else in the country/abroad.

At any time if my statement is found to be incorrect even after my graduation, the University has the right to withdraw my M.Phil Degree.

(Sajjad Hussain)

Registration No:MMT191007

Plagiarism Undertaking

I solemnly declare that research work presented in this thesis titled “**Heat and Mass Transfer Analysis of the Flow of a Williamson Nanofluid using Buongiorno Model**” is solely my research work with no significant contribution from any other person. Small contribution/help wherever taken has been dully acknowledged and that complete thesis has been written by me.

I understand the zero tolerance policy of the HEC and Capital University of Science and Technology towards plagiarism. Therefore, I as an author of the above titled thesis declare that no portion of my thesis has been plagiarized and any material used as reference is properly referred/cited.

I undertake that if I am found guilty of any formal plagiarism in the above titled thesis even after award of MPhil Degree, the University reserves the right to withdraw/revoke my M.Phil degree and that HEC and the University have the right to publish my name on the HEC/University website on which names of students are placed who submitted plagiarized work.

(Sajjad Hussain)

Registration No: MMT191007

Acknowledgement

I got no words to articulate my cordial sense of gratitude to **Almighty Allah** who is the most merciful and most beneficent to his creation.

I also express my gratitude to the last prophet of **Almighty Allah, Prophet Muhammad (PBUH)** the supreme reformer of the world and knowledge for human being.

I would like to be grateful to my thesis supervisor **Dr. Muhammad Sagheer**, the Head of the Department of Mathematics, for guiding and encouraging towards writing this thesis. It would have remained incomplete without his endeavours. Due to his efforts I was able to write and complete this assertion. Also special thanks to **Dr. Shafqat Hussain** for his valuable suggestions and co-operation and all other faculty members.

I would like to acknowledge the CUST for providing such a favourable environment for studies and thankful to all friends specially **Mr. Mehzad Ahmad** for their valuable suggestion and help during my research work.

I got no words to thank “**Al-Bader School**” and all staff specially **Col.(R) Zafar Asim** and **Mr. Asif Naveed Khan** for their encouragement and support during my studies.

I would like to be thankful to my uncles specially **Mr. Rehmat Hussain** for their support and encouragement during my studies.

I would like to pay great tribute to my parents, for their prayers, moral support and encouragement always push me to achieve my goals.

(Sajjad Hussain)

Abstract

The boundary layer flow of Williamson nanofluid over a stretching sheet with thermal and velocity slips is studied numerically. Buongiorno model is used to explore the heat transfer phenomena caused by Brownian motion and thermophoresis. The impact of MHD, Joule heating, porosity parameter and activation energy has been analyzed. Using similarity transformations, the governing equations are reduced to a set of nonlinear ordinary differential equations. These equations are solved numerically by using shooting method. The effects of non-Newtonian Williamson parameter, porosity parameter, activation energy, Joule heating, velocity and thermal slip parameters, Prandtl number, Brownian parameter, Schmidt number, Lewis number, Brownian motion parameter, thermophoresis parameter on velocity, temperature and concentration profile are shown in graphs and tables. The results reflect that the thickness of boundary layer decreases as the slip and thermal factor parameter increases. Further, the nanofluid temperature profile is enhanced with the raise of Williamson parameter, Eckert number, activation energy and Lewis number, while for the magnetic parameter, Prandtl number and thermal slip parameter, it is declined. The concentration profile is increased by accelerating value of the Williamson and Eckert number, however for the rising value of the magnetic and activation energy, the concentration profile is dropped.

Contents

Author's Declaration	iv
Plagiarism Undertaking	v
Acknowledgement	vi
Abstract	vii
List of Figures	x
List of Tables	xii
Abbreviations	xiii
Symbols	xiv
1 Literature Review	1
1.1 Introduction	1
1.2 Thesis Contributions	3
1.3 Layout of Thesis	4
2 Basic Terminologies and Laws	5
2.1 Some Basic Terminologies	5
2.2 Types of Fluids	7
2.3 Types of Flow	8
2.4 Modes of Heat Transfer	10
2.5 Dimensionless Numbers	11
2.6 Basic Principles of fluid flow	13
2.7 Governing Laws	13
3 Analysis of Williamson Nanofluid with Thermal and Velocity Slips for the Transfer of Heat and Mass	15
3.1 Introduction	15
3.2 Mathematical Modeling	15
3.3 Numerical Method for Solution	25

3.4	Representation of Graphs and Tables	28
4	Williamson Nanofluid flow with MHD, Porosity, Joule Heating and Activation Energy.	39
4.1	Introduction	39
4.2	Mathematical Modeling	39
4.3	Numerical Method for Solution	45
4.4	Representation of Graphs and Tables	48
5	Conclusion	61
	Bibliography	63

List of Figures

3.1	Geometric representation of the physical model.	16
3.2	Change in $f'(\eta)$ for rising value of δ	32
3.3	Change in $f'(\eta)$ for rising value of λ	32
3.4	Change in $\theta(\eta)$ for rising value of δ	33
3.5	Change in $\theta(\eta)$ for rising value of B	33
3.6	Change in $\theta(\eta)$ for rising value of λ	34
3.7	Change in $\theta(\eta)$ for rising value of Pr	34
3.8	Change in $\theta(\eta)$ for rising value of Nc	35
3.9	Change in $\theta(\eta)$ for rising value of Le	35
3.10	Change in $\theta(\eta)$ for rising value of Nbt	36
3.11	Change in $\phi(\eta)$ for rising value of δ	36
3.12	Change in $\phi(\eta)$ for rising value of B	37
3.13	Change in $\phi(\eta)$ for rising value of λ	37
3.14	Change in $\phi(\eta)$ for rising value of Nbt	38
3.15	Change in $\phi(\eta)$ for rising value of Sc	38
4.1	Geometric representation of the physical model.	40
4.2	Change in $f'(\eta)$ for rising value of δ	50
4.3	Effect of Williamson parameter λ on velocity profile $f'(\eta)$	52
4.4	Effect of porosity $k1$ on velocity profile $f'(\eta)$	52
4.5	Effect of Magnetic parameter M on velocity profile $f'(\eta)$	53
4.6	Effect of Eckert number E_c on temperature profile $\theta(\eta)$	53
4.7	Effect of magnetic parameter M on temperature profile $\theta(\eta)$	54
4.8	Effect of Prandtl number Pr on temperature profile $\theta(\eta)$	54
4.9	Effect of Lewis number on temperature profile $\theta(\eta)$	55
4.10	Effect of Thermophoretic parameter δ^* on temperature profile.	55
4.11	Effect of coefficient of activation energy $E1$ on temperature profile $\theta(\eta)$	56
4.12	Effect of temperature ratio parameter σ on temperature profile $\theta(\eta)$	56
4.13	Effect of diffusivity ratio parameter Nbt on temperature profile $\theta(\eta)$	57
4.14	Effect of thermal slip parameter β on temperature profile $\theta(\eta)$	57
4.15	Effect of Eckert number Ec on concentration profile $\phi(\eta)$	58
4.16	Effect of Prandtl number Pr on concentration profile $\phi(\eta)$	58
4.17	Effect of Magnetic parameter M on concentration profile $\phi(\eta)$	59
4.18	Effect of thermophoretic parameter δ^* on concentration profile $\phi(\eta)$	59

4.19	Effect of coefficient of activation energy E_1 on concentration profile $\phi(\eta)$	60
4.20	Effect of temperature ratio parameter σ on concentration profile $\phi(\eta)$	60

List of Tables

3.1	Impact of δ and λ on skin fraction	30
3.2	Effects of various parameters on Sherwood Number	30
3.3	Effects of various parameters on Nusselt Number	31
4.1	Effects of various parameters on skin fraction	50
4.2	Effects of various parameters on Nusselt Number and Sherwood Number	51

Abbreviations

IVPs	Initial values problems
MHD	Magneto-Hydrodynamics
ODEs	Ordinary differential equations
PDEs	Partial differential equations
RK	Runge-Kutta

Symbols

μ	Viscosity
ν	Kinematic viscosity
τ	Stress tensor
κ	Thermal conductivity
α	Thermal diffusivity
u	x-component of fluid velocity
y	y-component of fluid velocity
b	Strength of stagnation point flow
$T_w(x, t)$	Temperature of fluid near sheet
T_∞	Ambient Temperature
ρ	Density
ν_f	Kinematic viscosity of the base fluid
T	Temperature
σ^*	Stefan Boltzmann constant
k^*	Absorption coefficient
v_w	Suction/injection velocity
T_0, C_0	Positive reference temperature and nanoparticles volume fraction
ψ	Stream function
C_f	Skin friction coefficient
Nu_x	Local Nusselt number
Re_x	Local Reynolds number
Pr	Prandtl number
R	Thermal radiation parameter

η	Similarity variable
n	Stretching parameter
Ec	Eckert number

Chapter 1

Literature Review

1.1 Introduction

Many researchers have analyzed and determined a special kind of fluid having ideal properties and recognized as the suspended colloidal liquid having very small metallic or non-metallic particle called nanofluid. Buongiorno [1] found that the total velocity of nanoparticles look out as the sum of base fluid velocity and relative velocity. He examined seven slip components such as Newton's first law, Brownian dispersal, thermal diffusion, diffusiophoresis, magnetic impact, fluid drainage, and gravity settling. Analyzing every of these terms one by one, he stated that the Brownian dispersal and thermal diffusion is important when there is no existence of turbulent effect. The thermal conductivity of ordinary heat transfer fluids such as water, kerosene mineral oils and ethylene glycol rises by the inclusion of nanoparticles to a base fluid. Thus, there is no issue to use nanofluid as heat transfer fluid for cooling of electronics, automobile engine and vibrating heat pipes. Corcione et al. [2] used Buongiorno's work to examine natural convection flow of nanofluid's internal differentiable heated cavity and concluded that the dual phase combination technique is much reliable than the distinct phase model. A numerical study was conducted by Garoosi et al. [3] using Buongiorno's model. They examined natural and combine convection heat transfer of a nanofluid (Al_2O_3 -water) to one side inflamed quadrangle cavity. Eiamsa-ard et al.[4] found that in

a heat exchanger tube embellished with coinciding double warped-tape, the heat transfer of TiO_2 -water is accelerated. Outcomes of various papers show that for different nanofluids like AL_2O_3 -water and especially TiO_2 -water, the thermal diffusion force is essential. For such nanoparticles whose thermal conductivity is low, the thermal diffusion force is much essential. Many scholar's e.g namely Turkyilmazoglu [5], Qasim et al. [6], Hussanan et al. [7], Swalmeh et al. [8] and Afridi et al. [9] mentioned that the suspensions can increase thermal conductivity up to 20 percent even in the presence of low concentration nanofluid. An increase in the thermal conductivity mostly relies on different components such as size, shape, material and temperature of fluid particles, and so on. The objective of heat transfer coefficient is to obtain the components in forced convection cooling or heating application.

Krishnamurthy et al. [10], classified the Williamson nanofluid as an inelastic viscous fluid. The effect of velocity boundary layer on smooth flat surface was first time examined by Blasius [11]. Later on the theoretical features of estimated and exact techniques for the boundary layer on smooth surface was analyzed by Sakiadis [12]. Also, the convective boundary condition has been examined by Ramesh et al. [13] on Blasius and Sakiadis flows with the Williamson fluid. Preceding to that, Khan and Khan [14] used the homotopy analysis method (HAM) to examine the flow of Williamson fluid on boundary layer. He observed that by enhancing the Williamson parameter, the width of the boundary layer is reduced. Later on, Nadeem and Hussain [15] determined that the thermal conductivity of Williamson fluid become less than MHD Williamson nanofluid when it passes over the heated warm surface. Due to difference of temperature between objects, the thermal energy is caused. In various fields, heat transfer in non-Newtonian fluids has become common and essential. The issue of turbine cooling application with heat transfer in non-Newtonian inelastic viscous fluid was analyzed by Kurtcebe and Erim [16] concluded that the upper limit of inelastic viscous parameter relies on the Reynolds number. To obtain the best standard of the final products mostly in thermoplastic extrusion manufacture, the study of heat transfer flow in nanofluid over an elastic sheet is essential. The heat transfer and MHD boundary layer flow in nanofluid across a stretchable sheet was examined by Ibrahim and

Shankar [17]. Krishnamurthy et al. [18] using Williamson nanofluid, studied the consequences of chemical change on mollifying the heat transfer and magnetohydrodynamics boundary layer flow. At the same time, the flow characteristics and convective heat transfer of *Cu*-water nanofluids were analyzed by Xuan and Li [19]. Their analysis shows that, the heat transfer property enhances when volume fraction of nanoparticles rises. For identical Reynolds number, the swinging nanoparticles manifest greater heat transfer co-efficient and highly increase the heat transfer procedure contrast to the sub-structural fluid. Heris et al. [20] investigated the convective heat transfer resembling flow across the oxide nanofluid with boundary condition of constant wall temperature and finalized that there are many factors which increase the heat transfer such as disordered motion, thermal conductivity and instability of nanofluid. Slip condition plays a very important role in the interface of slip velocity between fluid and solid boundary in the presence of nanoparticles. Yang [21] expressed the viscous flow over a solid surface with slip boundary condition. The boundary relationship between fluid and solid is indicated by slip condition provided by the interaction of molecules and roughness of wall surface. The issue of the partial slip boundary condition influences on nanofluids with formulated wall temperature across a stretchable sheet was stated by Noghrehabadi et al. [22]. His results indicated that by increasing the velocity slip parameter, the Nusselt and Sherwood number are reduced. Malvandi et al. [23] carried out an experiment on the slip effects of nanofluids irregular immobility point over a stretching sheet. They observed that the value of skin friction decreases by increasing the values of the slip parameter. Numerically Raisi et al. [24] studied the slip and no slip conditions on the stratified nanofluids by forced convection. They found that the rate of heat transfer effects only higher Reynolds number as slip velocity coefficient increases. Keeping in view the above discussion our object is to analyze the slip conditions and heat transfer for Williamson nanofluid flowing across a stretchable sheet.

1.2 Thesis Contributions

The present work is focused on the numerical analysis of 2-D heat and mass transfer of the flow of a Williamson fluid with thermal and velocity slips and to analyze

the effect of magnetohydrodynamics, porosity parameter on velocity profile. Another purpose is to investigate the impact of Joule heating and activation energy on temperature and concentration profile respectively. The given non-linear PDEs are converted into system of ODEs by applying similarity transformations. Furthermore, for finding the numerical results of non-linear ODEs, the shooting technique is applied. The numerical results are computed by using MATLAB. The impact of significant parameters on $f'(\eta)$, $\theta(\eta)$, $\phi(\eta)$, skin friction Cf_x , Nusselt number Nu_x and Sherwood number Sh_x have been discussed through graphs and tables.

1.3 Layout of Thesis

A brief overview of the contents of the thesis is provided below.

Chapter 2 includes some basic definitions and terminologies, which are useful to understand the concepts discussed later on.

Chapter 3 provides the proposed analytical study of heat and mass transfer analysis of Williamson fluid over a non-linear stretching sheet. The numerical results of the governing flow equations are derived by using the shooting method.

Chapter 4 extends the flow model discussed in Chapter 3 by including MHD, porosity parameter, Joule heating and activation energy.

Chapter 5 provides the concluding remarks of the thesis.

References used in the thesis are mentioned in **Bibliography**.

Chapter 2

Basic Terminologies and Laws

In this chapter, some basic definitions, basic laws, terminologies and basic concepts of fluid dynamic have been presented. These concepts will be helpful to develop an understanding for the rest of the thesis.

2.1 Some Basic Terminologies

Definition 2.1.1 (Fluid)

“A fluid is a substance that deforms continuously under the application of a shear (tangential) stress no matter how small the shear stress may be.” [25]

Definition 2.1.2 (Mechanics)

“Mechanics is the oldest physical science that deals with both stationary and moving bodies under the influence of forces.” [26]

Definition 2.1.3 (Fluid Mechanics)

“Fluid mechanics is defined as the science that deals with the behavior of fluids at rest (fluid statics) or in motion (fluid dynamics), and the interaction of fluids with solids or other fluids at the boundaries.” [26]

Definition 2.1.4 (Dynamics)

“The branch of physics that deals with bodies in motion is called dynamics.” [26]

Definition 2.1.5 (Fluid Dynamics)

“ The study of fluids if the pressure forces are considered for the fluid in motion, that branch of science is called fluid dynamics.” [27]

Definition 2.1.6 (Statics)

“ The branch of mechanics that deals with bodies at rest is called statics.” [26]

Definition 2.1.7 (Fluid Statics)

“The study of fluids at rest is called fluid statics.” [27]

Definition 2.1.8 (Viscosity)

“Viscosity is that property of a fluid by virtue of which it offers resistance to the movement of one layer of fluid over an adjacent layer. It is primarily due to cohesion and molecular momentum exchange between fluid layers, and as flow occurs, these effects appear as shearing stresses between the moving layers of fluid. Mathematically,

$$\mu = \frac{\tau}{\frac{\partial u}{\partial y}},$$

where μ is viscosity coefficient, τ is shear stress and $\frac{\partial u}{\partial y}$ represents the velocity gradient.” [28]

Definition 2.1.9 (Kinematic Viscosity)

“It is defined as the ratio between the dynamic viscosity and density of fluid. It is denoted by symbol ν called **nu**. Mathematically,

$$\nu = \frac{\mu}{\rho}.” [27]$$

2.2 Types of Fluids

The fluids may be classified into the following types

Definition 2.2.1 (Ideal Fluids)

“A fluid, which is incompressible and has no viscosity, is known as an ideal fluid. Ideal fluid is only an imaginary fluid as all the fluids, which exist, have some viscosity.” [27]

Definition 2.2.2 (Real Fluids)

“A fluid, which possesses viscosity, is known as a real fluid. In actual practice, all the fluids are real fluids.” [27]

Definition 2.2.3 (Newtonian Fluids)

“A real fluid, in which the shear stress is directly proportional to the rate of shear strain (or velocity gradient), is known as a Newtonian fluid.” [27]

Definition 2.2.4 (Non-Newtonian Fluids)

“A real fluid in which the shear stress is not directly proportional to the rate of shear strain (or velocity gradient), is known as a non-Newtonian fluid.

$$\begin{aligned}\tau_{xy} &\propto \left(\frac{du}{dy}\right)^m, & m \neq 1 \\ \tau_{xy} &= \mu \left(\frac{du}{dy}\right)^m .” & [27]\end{aligned}$$

Definition 2.2.5 (Magnetohydrodynamics)

“Magnetohydrodynamics (MHD) is concerned with the mutual interaction of fluid flow and magnetic fields. The fluids in question must be electrically conducting and non-magnetic, which limits us to liquid metals, hot ionised gases (plasmas) and strong electrolytes.” [29]

2.3 Types of Flow

Definition 2.3.1 (Rotational Flow)

“A flow is said to be rotational if the fluid particles while moving in the direction of flow rotate about their mass centres.” [28]

Definition 2.3.2 (Irrotational Flow)

“A flow is said to be irrotational if the fluid particles while moving in the direction of flow do not rotate about their mass centres.” [28]

Definition 2.3.3 (Compressible Flow)

“Compressible flow is that type of flow in which the density of the fluid changes from point to point or in other words the density (ρ) is not constant for the fluid, Mathematically,

$$\rho \neq q,$$

where q is constant.” [27]

Definition 2.3.4 (Incompressible Flow)

“Incompressible flow is that type of flow in which the density is constant for the fluid. Liquids are generally incompressible while gases are compressible, Mathematically,

$$\rho = q,$$

where q is constant.” [27]

Definition 2.3.5 (Steady Flow)

“Fluid flow is said to be steady if at any point in the flowing fluid, various characteristics such as velocity, pressure, density, temperature etc., which describe the behaviour of the fluid in motion, do not change with time. Mathematically,

$$\frac{\partial Q}{\partial t} = 0,$$

where Q is any fluid property.” [28]

Definition 2.3.6 (Unsteady Flow)

“Fluid flow is said to be unsteady if at any point in the flowing fluid any one or

all the characteristics which describe the behavior of the fluid in motion change with time. Mathematically,

$$\frac{\partial Q}{\partial t} \neq 0,$$

where Q is any fluid property.” [28]

Definition 2.3.7 (Laminar Flow)

“ A flow is said to be laminar when various fluid particles move in layers (or laminae) with one layer of fluid sliding smoothly over an adjacent layer. Thus in the development of a laminar flow, the viscosity of the flowing fluid plays a significant role. As such the flow of a very viscous fluid may in general be treated as laminar flow.” [28]

Definition 2.3.8 (Turbulent Flow)

“ A fluid motion is said to be turbulent when the fluid particles move in an entirely haphazard or disorderly manner, that results in a rapid and continuous mixing of the fluid leading to momentum transfer as flow occurs.” [28]

Definition 2.3.9 (Uniform Flow)

“ When the velocity of flow of fluid does not change, both in magnitude and direction, from point to point in the flowing fluid, for any given instant of time, the flow is said to be uniform. Mathematically,

$$\left(\frac{\partial V}{\partial s} \right) = 0,$$

where V is called velocity.” [28]

Definition 2.3.10 (Non-uniform Flow)

“If the velocity of flow of fluid changes from point to point in the flowing fluid at any instant, the flow is said to be non-uniform. Mathematically,

$$\left(\frac{\partial V}{\partial s} \right) \neq 0,$$

where V is velocity.” [28]

Definition 2.3.11 (Internal Flow)

“Flows completely bounded by a solid surface are called internal or duct flows.” [25]

Definition 2.3.12 (External Flow)

“Flows over bodies immersed in an unbounded fluid are said to be an external flow.” [25]

2.4 Modes of Heat Transfer

Definition 2.4.1 (Heat Transfer)

“Thermal energy from a hot body flows to a cold body in the form of heat. This is called transfer of heat. Transfer of heat is a natural process. It continues all the time as long as the bodies in thermal contact are at different temperature.” [30]

Definition 2.4.2 (Conduction)

“The mode of transfer of heat by vibrating atoms and free electrons in solids from hot to cold parts of a body is called conduction of heat.” [30]

Example

”Touching a stove and being burned.

Ice cooling down your hand.

Definition 2.4.3 (Convection)

“Transfer of heat by actual movement of molecules from hot place to a cold place is known as convection.” [30]

Example

Hot air rising, cooling, and falling (convection currents).

Definition 2.4.4 (Radiation)

“Radiation is the mode of transfer of heat from one place to another in the form of waves, called electromagnetic waves. ” [30]

Example

Heat from the sun warming your face.

Definition 2.4.5 (Thermal Conductivity)

“The rate of flow of heat across the opposite faces of a metre cube of a substance maintained at a temperature difference of one kelvin is called the thermal conductivity of that substance. Mathematically,

$$k = \frac{Q}{t} \frac{L}{A(T_2 - T_1)}$$

where k is the proportionality constant called thermal conductivity of the solid.” [30]

Definition 2.4.6 (Thermal Diffusivity)

“The rate at which heat diffuses by conducting through a material depends on the thermal diffusivity and can be defined as,

$$\alpha = \frac{k}{\rho C_p},$$

where α is the thermal diffusivity, k is the thermal conductivity, ρ is the density and C_p is the specific heat at constant pressure.” [31]

2.5 Dimensionless Numbers

Definition 2.5.1 (Sherwood Number)

“It is a non dimensional quantity which shows the ratio of the mass transport by convection to the transfer of mass by diffusion. Mathematically,

$$Sh = \frac{kL}{D},$$

where L is characteristics length, D is the mass diffusivity and k is the mass transfer coefficient.” [32]

Definition 2.5.2 (Skin Friction Coefficient)

“The steady flow of an incompressible gas or liquid in a long pipe of internal diameter (D). The mean velocity is denoted by u_w . The skin friction coefficient can be defined as

$$C_f = \frac{2\tau_0}{\rho u_w^2}$$

where τ_0 denotes the wall shear stress and ρ is the density.” [33]

Definition 2.5.3 (Nusselt Number)

“The hot surface is cooled by a cold fluid stream. The heat from the hot surface, which is maintained at a constant temperature, is diffused through a boundary layer and convected away by the cold stream. Mathematically,

$$Nu = \frac{qL}{k}$$

where q stands for the convection heat transfer, L for the characteristic length and k stands for thermal conductivity.” [34]

Definition 2.5.4 (Eckert Number)

“It is a dimensionless number used in continuum mechanics. It describes the relation between flows and the boundary layer enthalpy difference and it is used for characterized heat dissipation. Mathematically,

$$Ec = \frac{u^2}{C_p \nabla T}$$

where C_p denotes the specific heat.” [25]

Definition 2.5.5 (Prandtl Number)

“It is the ratio between the momentum diffusivity ν and thermal diffusivity α . Mathematically, it can be defined as

$$Pr = \frac{\nu}{\alpha} = \frac{\frac{\mu}{\rho}}{\frac{k}{C_p \rho}} = \frac{\mu C_p}{k}$$

where μ represents the dynamic viscosity, C_p denotes the specific heat and k stands for thermal conductivity. The relative thickness of thermal and momentum boundary layer is controlled by Prandtl number. For small Pr , heat distributed rapidly corresponds to the momentum.” [25]

Definition 2.5.6 (Reynolds Number)

“It is defined as the ratio of inertia force of a flowing fluid and the viscous force of the fluid. Mathematically,

$$Re = \frac{VL}{\nu},$$

where U denotes the free stream velocity, L is the characteristic length and ν stands for kinematic viscosity.” [27]

Definition 2.5.6 (Schmidt Number)

“The number expressed the ratio of the kinematics viscosity or momentum transfer by internal friction to the molecular diffusivity. It characterized the relation between the material and momentum transfers in mass transfer.” [35]

2.6 Basic Principles of fluid flow

Difination 2.6.1 (Principle of conservation of mass)

“ The principle of conservation of mass states that mass can neither be created nor destroyed.” [28]

Difination 2.6.2 (Principle of Conservation of Energy)

“ The principle of conservation of energy states that energy can neither be created nor destroyed. ” [28]

Difination 2.6.3 (Principle of Conservation of Momentum)

“ The principle of conservation of momentum or impulse momentum principle states that the impulse of the resultant force, or the product of the force and time increment during which it acts, is equal to the change in the momentum of the body.” [28]

2.7 Governing Laws

Definition 2.7.1 (Continuity Equation)

“The continuity equation is actually a mathematical statement of the principle of conservation of mass. The most general expression on the basis of this principle may be obtained by considering a fixed region within a flowing fluid. Since fluid is neither created nor destroyed within a close region it may be stated that the rate of increase of the fluid mass contained within the region must be equal to the difference between the rate at which the fluid mass enters the region and the rate at which the fluid mass leaves the region. Mathematically, it can be written as

$$\frac{D\rho}{Dt} + \rho\nabla.V = 0." [28]$$

Definition 2.7.2 (Momentum Equation)

“This principle is a modified form of Newtons second law of motion. Newtons second law of motion states that the resultant external force acting on any body in any direction is equal to the rate of change of momentum of the body in that direction. Thus for any arbitrarily chosen direction x , it may be expressed as,

$$F_x = \frac{dM_x}{dt}$$

In which F_x represents the resultant external force in the x -direction and M_x represents the momentum in the x -direction. Above Equation may also be written as $F_x(dt) = d(M_x)$. The term $F_x(dt)$ is impulse and the term $d(M_x)$ is the resulting change of momentum.” [28]

Definition 2.7.3 (Energy Equation)

“The law of conservation of energy states that the time rate of change of the total energy is equal to the sum of the rate of work done by the applied forces and change of heat content per unit time.

$$\frac{\partial\rho}{\partial t} + \nabla.\rho\mathbf{u} = -\nabla.\mathbf{q} + Q + \phi,$$

where ϕ is the dissipation function.” [36]

Chapter 3

Analysis of Williamson Nanofluid with Thermal and Velocity Slips for the Transfer of Heat and Mass

3.1 Introduction

In this chapter, our aim is to study the flow of a 2-D Williamson nanofluid across a stretchable sheet and to analyze the computed results subject to the slip conditions. The set of non-linear PDEs is converted into the dimensionless ODEs by using some appropriate transformations. In order to solve ODEs, the shooting technique is implemented by using MATLAB. At the end of this chapter, the numerical solutions for different choices of various parameters will be analyzed for velocity, temperature and concentration profile. For a quantitative view, the obtained numerical findings are presented in tables and graphs.

3.2 Mathematical Modeling

In this section, we consider a 2-D flow of an incompressible Williamson nanofluid in steady state across a stretchable sheet. The linear stretching velocity of the

sheet has been taken as $U_w(x) = bx$, where b is a constant and x is the coordinate measure along the stretching sheet respectively. The y -axis has been taken perpendicular to the stretching sheet. The wall temperature is taken as $T_w = T_\infty + bx^2$, where T_∞ is the ambient temperature. The fluid's concentration at the sheet C_w is considered as constant throughout the stretching surface and when y continuously approaches to infinity, it approaches to C_∞ .

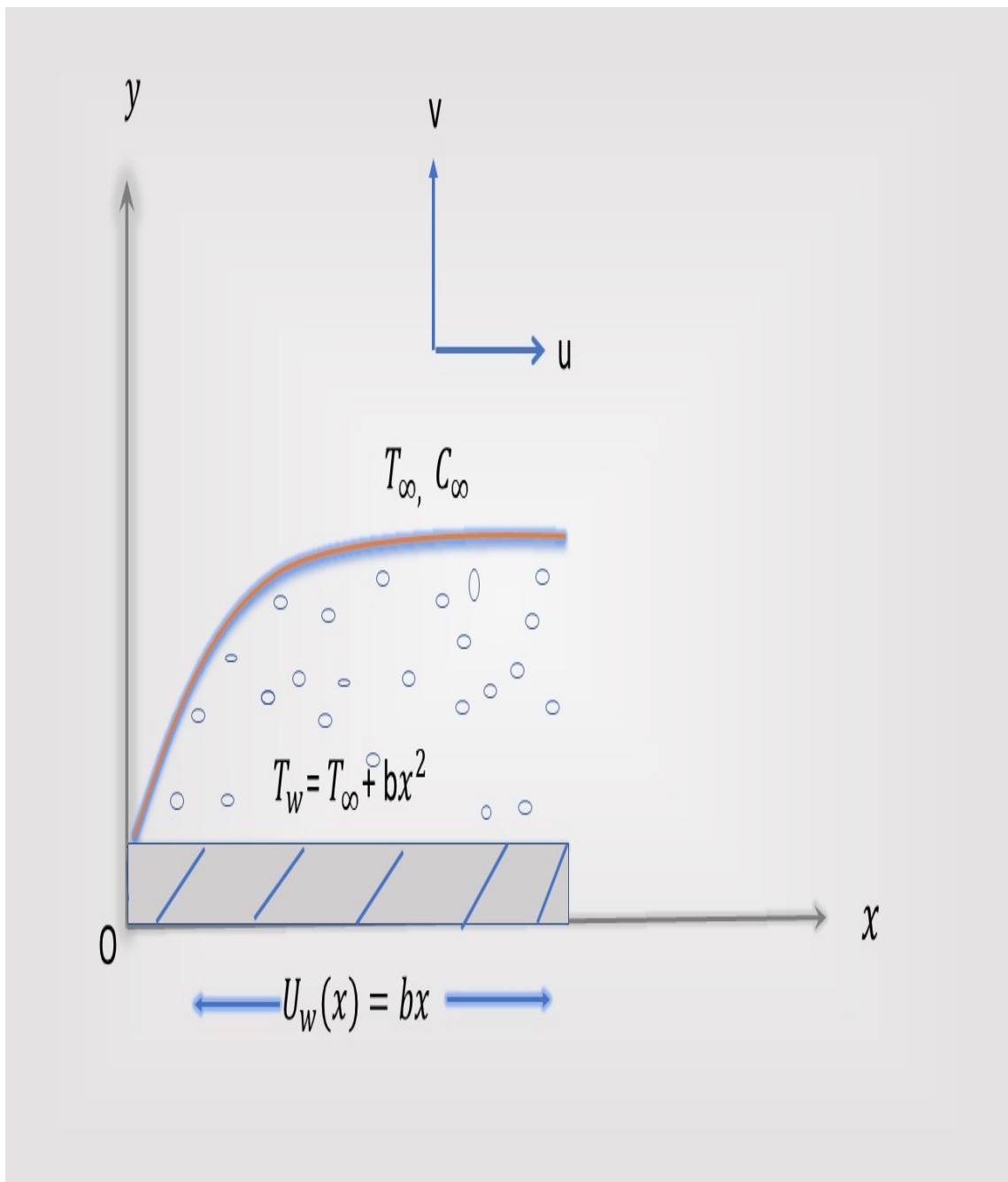


FIGURE 3.1: Geometric representation of the physical model.

The set of equations describing the non-Newtonian Williamson flow are as follows.

$$\frac{\partial u}{\partial x} + \frac{\partial v}{\partial y} = 0, \quad (3.1)$$

$$u \frac{\partial u}{\partial x} + v \frac{\partial u}{\partial y} = \nu \frac{\partial^2 u}{\partial y^2} + \sqrt{2\nu}\Gamma \frac{\partial u}{\partial y} \frac{\partial^2 u}{\partial y^2}, \quad (3.2)$$

$$u \frac{\partial T}{\partial x} + v \frac{\partial T}{\partial y} = \alpha \left(\frac{\partial^2 T}{\partial y^2} \right) + \frac{\rho_p C_p}{\rho C} \left[D_B \frac{\partial C}{\partial y} \frac{\partial T}{\partial y} + \frac{D_T}{T_\infty} \left(\frac{\partial T}{\partial y} \right)^2 \right], \quad (3.3)$$

$$u \frac{\partial C}{\partial x} + v \frac{\partial C}{\partial y} = D_B \frac{\partial^2 C}{\partial y^2} + \frac{D_T}{T_\infty} \frac{\partial^2 T}{\partial y^2}. \quad (3.4)$$

The associated BCs have been taken as

$$\left. \begin{aligned} u &= u_w + \delta^* \mu \left(\frac{\partial u}{\partial y} \right), \quad v = 0, \quad T = T_w + B * \frac{\partial T}{\partial y}, \quad C = C_w, \quad \text{at } y = 0, \\ u &\rightarrow 0, \quad T \rightarrow T_\infty, \quad C = C_\infty, \quad \text{as } y \rightarrow \infty. \end{aligned} \right\} \quad (3.5)$$

To convert equations (3.1)-(3.4) into a system of ODEs, the following similarity transformations [32] will be used.

$$\left. \begin{aligned} u &= bx f'(\eta), \quad v = -(b\nu)^{\frac{1}{2}} f(\eta), \quad \eta = \sqrt{\frac{b}{\nu}} y, \\ \theta(\eta) &= \frac{T - T_\infty}{T_w - T_\infty}, \quad \phi(\eta) = \frac{C - C_\infty}{C_w - C_\infty} \end{aligned} \right\} \quad (3.6)$$

For the conversion of equations (3.1)-(3.4) into the dimensionless form, the detailed procedure has been discussed as bellow.

- $u = bx f'(\eta),$
 $\frac{\partial u}{\partial x} = \frac{\partial}{\partial x} (bx f'(\eta)),$
 $= b f'(\eta)$. (3.7)

$$\begin{aligned} u \frac{\partial u}{\partial x} &= bx f'(\eta) (b f'(\eta)), \\ &= b^2 x f'^2(\eta). \end{aligned} \quad (3.8)$$

$$\frac{\partial u}{\partial y} = bx f''(\eta) \sqrt{\frac{b}{\nu}}, \quad (3.9)$$

$$v \frac{\partial u}{\partial y} = -\sqrt{b\nu} f(\eta) bx f''(\eta) \sqrt{\frac{b}{\nu}},$$

$$= -b^2 x f(\eta) f''(\eta). \quad (3.10)$$

$$\begin{aligned} \frac{\partial^2 u}{\partial y^2} &= b x f''' \frac{b}{\nu}, \\ &= \frac{b^2 x}{\nu} f''', \\ \nu \frac{\partial^2 u}{\partial y^2} &= b^2 x f'''. \end{aligned} \quad (3.11)$$

- $v = -\sqrt{b\nu} f(\eta).$

$$\begin{aligned} \frac{\partial v}{\partial y} &= -\sqrt{b\nu} f'(\eta) \sqrt{\frac{b}{\nu}} \\ &= -b f'(\eta). \end{aligned} \quad (3.12)$$

- $\theta(\eta) = \frac{T - T_\infty}{T_w - T_\infty}.$

$$T = \theta(\eta)(T_w - T_\infty) + T_\infty. \quad (3.13)$$

$$\begin{aligned} \frac{\partial T}{\partial x} &= 0. \\ u \frac{\partial T}{\partial x} &= 0. \end{aligned} \quad (3.14)$$

$$\frac{\partial T}{\partial y} = (T_w - T_\infty) \theta'(\eta) \sqrt{\frac{b}{\nu}}. \quad (3.15)$$

$$\begin{aligned} v \frac{\partial T}{\partial y} &= -\sqrt{b\nu} f(\eta) (T_w - T_\infty) \theta'(\eta) \sqrt{\frac{b}{\nu}} \\ &= -b(T_w - T_\infty) f(\eta) \theta'(\eta). \end{aligned} \quad (3.16)$$

$$\begin{aligned} \frac{\partial^2 T}{\partial y^2} &= (T_w - T_\infty) \theta''(\eta) \sqrt{\frac{b}{\nu}} \sqrt{\frac{b}{\nu}}, \\ &= \frac{b}{\nu} (T_w - T_\infty) \theta''(\eta). \end{aligned} \quad (3.17)$$

- $\phi(\eta) = \frac{C - C_\infty}{C_w - C_\infty}.$

$$\Rightarrow C = \phi(\eta)(C_w - C_\infty) + C_\infty. \quad (3.18)$$

$$\begin{aligned} \frac{\partial C}{\partial x} &= 0. \\ u \frac{\partial C}{\partial x} &= 0. \end{aligned} \quad (3.19)$$

$$\frac{\partial C}{\partial y} = (C_w - C_\infty) \phi'(\eta) \sqrt{\frac{b}{\nu}}. \quad (3.20)$$

$$\begin{aligned} v \frac{\partial C}{\partial y} &= -\sqrt{b\nu} f(\eta) (C_w - C_\infty) \phi'(\eta) \sqrt{\frac{b}{\nu}} \\ &= -b(C_w - C_\infty) f(\eta) \phi'(\eta). \end{aligned} \quad (3.21)$$

$$\frac{\partial^2 C}{\partial y^2} = (C_w - C_\infty)\phi''(\eta)\frac{b}{\nu}. \quad (3.22)$$

We can easily satisfy equation (3.1) by using the above equations (3.7) and (3.12), as follows

$$\begin{aligned} \frac{\partial u}{\partial x} + \frac{\partial v}{\partial y} &= bf'(\eta) - bf'(\eta), \\ \frac{\partial u}{\partial x} + \frac{\partial v}{\partial y} &= 0. \end{aligned} \quad (3.23)$$

Now, to convert the momentum equation (3.2), into the dimensionless form we will use equations (3.8) and (3.9) in the left side of equation (3.2) as below

$$\begin{aligned} u\frac{\partial u}{\partial x} + v\frac{\partial u}{\partial y} &= b^2xf'^2(\eta) + (-b^2xf(\eta)f''(\eta)), \\ &= b^2xf'^2(\eta) - b^2xf(\eta)f''(\eta), \\ &= b^2x(f'^2(\eta) - f(\eta)f''(\eta)). \end{aligned} \quad (3.24)$$

Using (3.9) and (3.11), in the right side of equation (3.2) it becomes

$$\begin{aligned} \nu\frac{\partial^2 u}{\partial y^2} + \sqrt{2}\nu\Gamma\frac{\partial u}{\partial y}\frac{\partial^2 u}{\partial y^2} &= b^2xf''' + \sqrt{2}\Gamma(bxf''\sqrt{\frac{b}{\nu}})(b^2xf'''). \\ \Rightarrow \nu\frac{\partial^2 u}{\partial y^2} + \sqrt{2}\nu\Gamma\frac{\partial u}{\partial y}\frac{\partial^2 u}{\partial y^2} &= b^2xf''' + \sqrt{2}\Gamma b^2x^2\sqrt{\frac{b^3}{\nu}}f''f'''. \end{aligned} \quad (3.25)$$

By comparing (3.24) and (3.25), the dimensionless form of (3.2), is given by

$$\begin{aligned} b^2xf'^2(\eta) - b^2xf(\eta)f''(\eta) &= b^2xf''' + \sqrt{2}x\Gamma b^2x^2\sqrt{\frac{b^3}{\nu}}f''f'''. \\ \Rightarrow b^2x(f'^2(\eta) - f(\eta)f''(\eta)) &= b^2x\left(f''' + \sqrt{2}x\Gamma\sqrt{\frac{b^3}{\nu}}f''f'''\right). \\ \Rightarrow f'^2(\eta) - f(\eta)f''(\eta) &= f'''(\eta) + \sqrt{2}x\Gamma\sqrt{\frac{b^3}{\nu}}f''f'''(\eta). \\ \Rightarrow f'''(\eta) + \sqrt{2}x\Gamma\sqrt{\frac{b^3}{\nu}}f''f'''(\eta) + f(\eta)f''(\eta) - f'^2(\eta) &= 0. \\ \Rightarrow f'''(\eta) + \lambda f''(\eta)f'''(\eta) + f(\eta)f''(\eta) - f'^2(\eta) &= 0, \end{aligned} \quad (3.26)$$

where $\lambda = \sqrt{2}x\Gamma\sqrt{\frac{b^3}{\nu}}$ is called non-Newtonian Williamson parameter.

Now, to convert equation (3.3) into the dimensionless form, we will use equations (3.14) and (3.16) in left side of (3.3), to get

$$\begin{aligned} u \frac{\partial T}{\partial x} + v \frac{\partial T}{\partial y} &= 0 - b(T_w - T_\infty) f(\eta) \theta'(\eta), \\ &= -b(T_w - T_\infty) f(\eta) \theta'(\eta). \end{aligned} \quad (3.27)$$

Now, using equations (3.15), (3.17) and (3.19) in the right hand side of equation (3.3), we get

$$\begin{aligned} \alpha \left(\frac{\partial^2 T}{\partial y^2} \right) + \frac{\rho_p C_p}{\rho C} \left[D_B \frac{\partial C}{\partial y} \frac{\partial T}{\partial y} + \frac{D_T}{T_\infty} \left(\frac{\partial T}{\partial y} \right)^2 \right] &= \alpha \frac{b}{\nu} (T_w - T_\infty) \theta''(\eta) + \\ \frac{\rho_p C_p}{\rho C} D_B (T_w - T_\infty) (C_w - C_\infty) \theta'(\eta) \phi'(\eta) \frac{b}{\nu} + \frac{\rho_p C_p}{\rho C} \frac{D_T}{T_\infty} \left(\frac{b}{\nu} (T_w - T_\infty)^2 \theta'^2(\eta) \right). \end{aligned} \quad (3.28)$$

By comparing equation (3.27) and (3.28), we can obtain the dimensionless form of equation (3.3), which is as below.

$$\begin{aligned} -b(T_w - T_\infty) f(\eta) \theta'(\eta) &= \alpha \frac{b}{\nu} (T_w - T_\infty) \theta''(\eta) \\ &+ \frac{\rho_p C_p}{\rho C} D_B (T_w - T_\infty) (C_w - C_\infty) \theta'(\eta) \phi'(\eta) \frac{b}{\nu} \\ &+ \frac{\rho_p C_p}{\rho C} \frac{D_T}{T_\infty} \left(\frac{b}{\nu} (T_w - T_\infty)^2 \theta'^2(\eta) \right). \\ \Rightarrow \alpha \frac{b}{\nu} (T_w - T_\infty) \theta''(\eta) + \frac{\rho_p C_p}{\rho C} D_B (T_w - T_\infty) (C_w - C_\infty) \theta'(\eta) \phi'(\eta) \frac{b}{\nu} \\ &+ \frac{\rho_p C_p}{\rho C} \frac{D_T}{T_\infty} \left(\frac{b}{\nu} (T_w - T_\infty)^2 \theta'^2(\eta) \right) + b(T_w - T_\infty) f(\eta) \theta'(\eta) = 0. \\ \Rightarrow \alpha \frac{b}{\nu} (T_w - T_\infty) \left(\theta''(\eta) + \frac{\nu}{\alpha} f(\eta) \theta'(\eta) + \frac{\rho_p C_p}{\rho C} \frac{D_B}{\alpha} (C_w - C_\infty) \theta'(\eta) \phi'(\eta) \right) \\ &+ \alpha \frac{b}{\nu} (T_w - T_\infty) \left(\frac{\rho_p C_p}{\rho C} \frac{D_T}{T_\infty} (T_w - T_\infty) \theta'^2(\eta) \right) = 0. \\ \Rightarrow \theta''(\eta) + \frac{\nu}{\alpha} f(\eta) \theta'(\eta) + \frac{\rho_p C_p}{\rho C} \frac{D_B}{\alpha} (C_w - C_\infty) \theta'(\eta) \phi'(\eta) \\ &+ \frac{\rho_p C_p}{\rho C} \frac{D_T}{T_\infty} (T_w - T_\infty) \theta'^2(\eta) = 0. \\ \Rightarrow \theta''(\eta) + Pr f(\eta) \theta'(\eta) + \frac{Nc}{Le} \theta'(\eta) \phi'(\eta) + \frac{Nc}{Le Nb t} \theta'^2(\eta) = 0, \end{aligned} \quad (3.29)$$

where $Pr = \frac{\nu}{\alpha}$ is Prandtl number, $Nc = \frac{\rho_p C_p}{\rho C} (C_w - C_\infty)$, is the heat capacity ratio parameter, $Le = \frac{D_B}{\alpha}$ is the Lewis number and $Nbt = \frac{\rho_p C_p}{\rho C} \frac{D_T}{T_\infty} \frac{(C_w - C_\infty)}{(T_w - T_\infty)}$ is the diffusivity ratio parameter.

Now, using equations (3.19) and (3.21) in the left side of equation (3.4), it is converted into the following dimensionless form.

$$\begin{aligned} u \frac{\partial C}{\partial x} + v \frac{\partial C}{\partial y} &= 0 - b(C_w - C_\infty) f(\eta) \phi'(\eta), \\ &= -b(C_w - C_\infty) f(\eta) \phi'(\eta). \end{aligned} \quad (3.30)$$

Using equations (3.17) and (3.22) in the right hand side of equation (3.4), we get

$$D_B \frac{\partial^2 C}{\partial y^2} + \frac{D_T}{T_\infty} \frac{\partial^2 T}{\partial y^2} = D_B \frac{b}{\nu} (C_w - C_\infty) \phi''(\eta) + \frac{D_T}{T_\infty} \frac{b}{\nu} (T_w - T_\infty) \theta''(\eta). \quad (3.31)$$

By comparing equation (3.30) and (3.31), we can obtain the dimensionless form of equation (3.4), which is

$$\begin{aligned} -b(C_w - C_\infty) f(\eta) \phi'(\eta) &= D_B \frac{b}{\nu} (C_w - C_\infty) \phi''(\eta) + \frac{D_T}{T_\infty} \frac{b}{\nu} (T_w - T_\infty) \theta''(\eta). \\ \Rightarrow D_B \frac{b}{\nu} (C_w - C_\infty) \phi''(\eta) + \frac{D_T}{T_\infty} \frac{b}{\nu} (T_w - T_\infty) \theta''(\eta) + b(C_w - C_\infty) f(\eta) \phi'(\eta) &= 0. \\ \Rightarrow D_B \frac{b}{\nu} (C_w - C_\infty) \left(\phi''(\eta) + \frac{D_T}{T_\infty D_B} \frac{(T_w - T_\infty)}{(C_w - C_\infty)} \theta''(\eta) + \frac{\nu}{D_B} f(\eta) \phi'(\eta) \right) &= 0. \\ \Rightarrow \phi''(\eta) + \frac{\nu}{D_B} f(\eta) \phi'(\eta) + \frac{D_T}{T_\infty D_B} \frac{(T_w - T_\infty)}{(C_w - C_\infty)} \theta''(\eta) &= 0. \\ \Rightarrow \phi''(\eta) + Sc f(\eta) \phi'(\eta) + \frac{1}{Nbt} \theta''(\eta) &= 0. \end{aligned} \quad (3.32)$$

Here $Sc = \frac{\nu}{D_B}$ is called Schmidt number and $Nbt = \frac{T_\infty D_B}{D_T} \frac{(C_w - C_\infty)}{(T_w - T_\infty)}$ is called diffusivity ratio parameter.

Now, for the conversion of boundary conditions into the dimensionless form we follow the procedure shown as below

- $u = u_w + \delta^* \mu \frac{\partial u}{\partial y},$ at $y = 0.$
- $\Rightarrow bx f'(\eta) = bx + \delta^* \mu bx f''(\eta) \sqrt{\frac{b}{\nu}},$ at $\eta = 0$

$$\begin{aligned} \Rightarrow \quad bx f'(\eta) &= bx \left(1 + \delta^* \mu f''(\eta) \sqrt{\frac{b}{\nu}} \right), & \text{at } \eta = 0. \\ \Rightarrow \quad f'(\eta) &= 1 + \delta^* \mu f''(\eta) \sqrt{\frac{b}{\nu}}, & \text{at } \eta = 0. \\ \Rightarrow \quad f'(\eta) &= 1 + \delta f''(\eta), & \text{at } \eta = 0. \\ \Rightarrow \quad f'(0) &= 1 + \delta f''(0), & \text{at } \eta = 0. \\ \bullet \quad T &= T_w + B^* \frac{\partial T}{\partial y}, & \text{at } y = 0. \\ \Rightarrow \quad \theta(\eta)(T_w - T_\infty) + T_\infty &= ax^2 + T_\infty + B^* \frac{\partial T}{\partial y}, & \text{at } \eta = 0. \\ \Rightarrow \quad \theta(\eta)(T_w - T_\infty) &= ax^2 + B^* \theta'(\eta)(T_w - T_\infty) \sqrt{\frac{b}{\nu}}, & \text{at } \eta = 0. \\ \Rightarrow \quad \theta(\eta)(bx^2 + T_\infty - T_\infty) &= ax^2 + B^* \theta'(\eta)(bx^2 + T_\infty - T_\infty) \sqrt{\frac{b}{\nu}}, & \text{at } \eta = 0. \\ \Rightarrow \quad \theta(\eta)(bx^2) &= ax^2 + B^* \theta'(\eta) bx^2 \sqrt{\frac{b}{\nu}}, & \text{at } \eta = 0. \\ \Rightarrow \quad bx^2 \theta(\eta) &= ax^2 \left(1 + B^* \sqrt{\frac{b}{\nu}} \theta'(\eta) \right), & \text{at } \eta = 0. \\ \Rightarrow \quad \theta(\eta) &= \left(1 + B^* \sqrt{\frac{b}{\nu}} \theta'(\eta) \right), & \text{at } \eta = 0. \\ \Rightarrow \quad \theta(\eta) &= (1 + \beta \theta'(\eta)), & \text{at } \eta = 0. \\ \Rightarrow \quad \theta(0) &= (1 + \beta \theta'(0)), & \text{at } \eta = 0. \\ \bullet \quad C &= C_w, & \text{at } y = 0. \\ \Rightarrow \quad \phi(\eta)(C_w - C_\infty) + C_\infty &= C_w, & \text{at } \eta = 0. \\ \Rightarrow \quad \phi(\eta) &= \frac{C_w - C_\infty}{C_w - C_\infty}, & \text{at } \eta = 0. \\ \Rightarrow \quad \phi(0) &= 1, & \text{at } \eta = 0. \\ \bullet \quad v &= 0, & \text{at } y = 0. \\ \Rightarrow \quad -(b\nu)^{\frac{1}{2}} f(\eta) &= 0, & \text{at } \eta = 0. \\ \Rightarrow \quad f(\eta) &= 0, & \text{at } \eta = 0. \\ \Rightarrow \quad f(0) &= 0, & \text{at } \eta = 0. \\ \bullet \quad u &\rightarrow 0, & \text{as } y \rightarrow \infty. \\ \Rightarrow \quad af'(\eta)x^2 &\rightarrow 0, & \text{as } \eta \rightarrow \infty. \\ \Rightarrow \quad f'(\eta) &\rightarrow 0, & \text{as } \eta \rightarrow \infty. \\ \bullet \quad T &\rightarrow T_\infty & \text{as } y \rightarrow \infty. \end{aligned}$$

$$\begin{aligned}
 &\Rightarrow \theta(\eta)(T_w - T_\infty) + T_\infty \rightarrow T_\infty, && \text{as } \eta \rightarrow \infty. \\
 &\Rightarrow \theta(\eta)(T_w - T_\infty) \rightarrow 0, && \text{as } \eta \rightarrow \infty. \\
 &\Rightarrow \theta(\eta) \rightarrow 0, && \text{as } \eta \rightarrow \infty. \\
 \bullet & \quad C \rightarrow C_\infty && \text{as } y \rightarrow \infty. \\
 &\Rightarrow \phi(\eta)(C_w - C_\infty) + C_\infty \rightarrow C_\infty, && \text{as } \eta \rightarrow \infty. \\
 &\Rightarrow \phi(\eta)(C_w - C_\infty) \rightarrow 0, && \text{as } \eta \rightarrow \infty. \\
 &\Rightarrow \phi(\eta) \rightarrow 0, && \text{as } \eta \rightarrow \infty.
 \end{aligned}$$

The final dimensionless form of the governing model, is

$$f'''(\eta) + \lambda f''(\eta)f'''(\eta) + f(\eta)f''(\eta) - f'^2(\eta) = 0. \tag{3.33}$$

$$\theta''(\eta) + Pr f(\eta)\theta'(\eta) + \frac{Nc}{Le}\theta'(\eta)\phi'(\eta) + \frac{Nc}{LeNbt}\theta'^2(\eta) = 0. \tag{3.34}$$

$$\phi''(\eta) + Sc f(\eta)\phi'(\eta) + \frac{1}{Nbt}\theta''(\eta) = 0. \tag{3.35}$$

The associated BCs (3.5) in the dimensionless form are

$$\left. \begin{aligned}
 f(\eta) = 0, \quad f'(\eta) = 1 + \delta f''(\eta), \quad \theta(\eta) = 1 + \beta\theta'(\eta), \quad \phi(\eta) = 1 \quad \text{at } \eta = 0 \\
 f'(\eta) = 0, \quad \theta(\eta) = 0, \quad \phi(\eta) = 0 \quad \text{as } \eta \rightarrow \infty.
 \end{aligned} \right\} \tag{3.36}$$

The skin friction coefficient, is given as follows

$$C_f = \frac{\tau_w}{\rho U_w^2(x)}. \tag{3.37}$$

$$\tau_w = \mu \left[\frac{\partial u}{\partial y} + \frac{\Gamma}{\sqrt{2}} \left(\frac{\partial u}{\partial y} \right)^2 \right]. \tag{3.38}$$

Therefore, the dimensionless form of C_f is

$$C_f = \frac{\mu \left[\frac{\partial u}{\partial y} + \frac{\Gamma}{\sqrt{2}} \left(\frac{\partial u}{\partial y} \right)^2 \right]}{\rho U_w(x)^2},$$

$$\begin{aligned}
 &= \frac{\mu \left(bx f''(\eta) \sqrt{\frac{b}{\nu}} + \frac{\Gamma}{\sqrt{2}} b^2 x^2 f''^2 \frac{b}{\nu} \right)}{\rho b^2 x^2}, \\
 &= \frac{\nu \rho \left(bx \sqrt{\frac{b}{\nu}} \left(f''(\eta) + \frac{\Gamma}{\sqrt{2}} bx \sqrt{\frac{b}{\nu}} f''^2 \right) \right)}{\rho b^2 x^2}, \\
 &= \frac{\nu \sqrt{\frac{b}{\nu}} \left(f''(\eta) + \frac{\Gamma}{\sqrt{2}} bx \sqrt{\frac{b}{\nu}} f''^2 \right)}{bx}, \\
 &= \frac{\nu \sqrt{\frac{b}{\nu}} \left(f''(\eta) + \frac{\Gamma}{\sqrt{2}} bx \sqrt{\frac{b}{\nu}} f''^2 \right)}{bx}, \\
 \Rightarrow C_f \sqrt{\frac{b}{\nu}} x &= \left(f''(\eta) + \sqrt{\frac{2b^3}{\nu}} \Gamma x f''^2 \right). \\
 \Rightarrow C_f \sqrt{Re} &= \left(f''(\eta) + \frac{\lambda}{\sqrt{2}} f''^2 \right), \tag{3.39}
 \end{aligned}$$

where Re denotes the Reynolds number defined as $Re = \frac{b}{\nu} x^2$.

Now, Local Nusselt number is defined as follow

$$Nu = \frac{xq_w}{k(T_w - T_\infty)}. \tag{3.40}$$

To achieve the dimensionless form of Nu , the following formula will be helpful.

$$q_w = -k \left(\frac{\partial T}{\partial y} \right)_{y=0}. \tag{3.41}$$

Using equation (3.41), in equation (3.40) we get the following form

$$\begin{aligned}
 Nu &= \frac{-xk \left(\frac{\partial T}{\partial y} \right)_{y=0}}{k(T_w - T_\infty)}, \\
 &= \frac{-x \left(\sqrt{\frac{b}{\nu}} (T_w - T_\infty) \theta'(\eta) \right)_{y=0}}{(T_w - T_\infty)}, \\
 &= -x \left(\sqrt{\frac{b}{\nu}} \theta'(\eta) \right)_{y=0}, \\
 &= -x \sqrt{\frac{b}{\nu}} \theta'(0), \\
 &= \sqrt{Re} \theta'(0).
 \end{aligned}$$

$$\Rightarrow \frac{Nu}{\sqrt{Re}} = \theta'(0). \quad (3.42)$$

Now, Sherwood number is defined as follow

$$Sh = \frac{xq_m}{D_B(C_w - C_\infty)}. \quad (3.43)$$

Since

$$q_m = -D_B \left(\frac{\partial C}{\partial y} \right)_{y=0}, \quad (3.44)$$

therefore, the dimensionless form of Sh is

$$\begin{aligned} Sh &= \frac{-xD_B \left(\frac{\partial C}{\partial y} \right)_{y=0}}{D_B(C_w - C_\infty)}, \\ &= \frac{-x \left((C_w - C_\infty) \sqrt{\frac{b}{\nu}} \phi'(\eta) \right)_{y=0}}{(C_w - C_\infty)}, \\ &= -x \left(\sqrt{\frac{b}{\nu}} \phi'(\eta) \right)_{y=0}, \\ &= -\sqrt{Re} \phi'(0). \end{aligned}$$

$$\Rightarrow \frac{Sh}{\sqrt{Re}} = -\phi'(0). \quad (3.45)$$

3.3 Numerical Method for Solution

The shooting method has been used to solve the ordinary differential equation (3.33). The following notations have been considered.

$$f = y_1, \quad f' = y_1' = y_2, \quad f'' = y_1'' = y_2' = y_3, \quad f''' = y_3'.$$

As a result, the momentum equation is converted into the following system of first order ODEs.

$$\begin{aligned}
 y_1' &= y_2, & y_1(0) &= 0, \\
 y_2' &= y_3, & y_2(0) &= 1 + \delta T, \\
 y_3' &= \frac{1}{1 + \lambda y_3}(y_2^2 - y_3 y_1), & y_3(0) &= T,
 \end{aligned}$$

The above initial value problem (IVP) will be numerically solved by RK-4 method. For the numerical solution, the unbounded domain $[0, \infty [$ has been replaced by $[0, \eta_\infty]$ where η_∞ is a real number having the property that for $\eta > \eta_\infty$, there is no significant variation in the solution. In this initial value problem, the missing condition g is to be chosen such that

$$y_2(\eta_\infty, g) = 0,$$

For the convenience, let us denote $y_2(\eta_\infty, g)$ by $y_2(g)$. Such notations will also be used for all y_i or their derivatives, where $i = 1, 2, 3, 4, 5, 6$

To find g we will use Newton's method which has the following iterative scheme.

$$g^{n+1} = g^n - \frac{y_2(g^n)}{\left(\frac{\partial y_2}{\partial g}\right)_{g=g^n}}$$

We further introduce, the following notations to obtain the derivative $\left(\frac{\partial y_2}{\partial g}\right)_{g=g^n}$

$$\frac{\partial y_1}{\partial g} = y_4, \quad \frac{\partial y_2}{\partial g} = y_5, \quad \frac{\partial y_3}{\partial g} = y_6.$$

By differentiating the last system of ODEs with respect to g , we get.

$$\begin{aligned}
 y_4' &= y_5, & y_4(0) &= 0, \\
 y_5' &= y_6, & y_5(0) &= 0, \\
 y_6' &= \frac{2y_5 y_2 - y_1 y_6 - y_3 y_6 + 2\lambda y_2 y_3 y_5 - \lambda y_3^2 y_4 - \lambda y_2^2 y_6}{(1 + \lambda y_3)^2} & y_6(0) &= 1.
 \end{aligned}$$

The stopping criteria for the Newton's technique, is set as

$$| y_2(g) | < \epsilon,$$

where $\epsilon > 0$ is an arbitrarily small positive number. From now onward ϵ has been

taken as 10^{-10} .

The equation (3.34) and equation (3.35) are coupled equations will be solved numerically by using the shooting method by assuming f as a known function. For this we use the following notions

$$\theta = Y_1, \quad \theta' = Y_2, \quad \theta'' = Y_2'$$

$$\phi = Y_3, \quad \phi' = Y_4, \quad \phi'' = Y_4'$$

The system of equation (3.34) and (3.35) can be written in the form of the following first order coupled ODEs.

$$Y_1' = Y_2, \quad Y_1(0) = 1 + Bq,$$

$$Y_2' = - \left(P_r C_1 y_2 + \frac{Nc}{Le} Y_2 Y_4 + \frac{Nc}{L_e N_{bt}} Y_2^2 \right), \quad Y_2(0) = q,$$

$$Y_3' = Y_4, \quad Y_3(0) = 1.$$

$$Y_4' = -ScC_1 Y_4 + \frac{1}{N_{bt}} \left(P_r C_1 Y_2 + \frac{Nc}{Le} Y_2 Y_4 + \frac{Nc}{L_e N_{bt}} Y_2^2 \right), \quad Y_4(0) = r.$$

The RK-4 method has been taken into consideration for solving the above initial value problem. For the above system of equations, the missing conditions are to be chosen such that

$$Y_1(q, r) = 0, \quad Y_3(q, r) = 0.$$

Note that $Y_i(q, r)$ and their partial derivatives w.r.t q and r at $\eta = \eta_\infty$ will be denoted by $Y_i(q, r)$, $\frac{\partial Y_i}{\partial q}$, and $\frac{\partial Y_i}{\partial r}$, where $i = 1, 2, 3, \dots, 12$

To solve the above algebraic equations, we apply the Newton's method.

$$\begin{bmatrix} q^{n+1} \\ r^{n+1} \end{bmatrix} = \begin{bmatrix} q^n \\ r^n \end{bmatrix} - \left(\begin{bmatrix} \frac{\partial Y_1}{\partial q} & \frac{\partial Y_1}{\partial r} \\ \frac{\partial Y_3}{\partial q} & \frac{\partial Y_3}{\partial r} \end{bmatrix}^{-1} \begin{bmatrix} Y_1 \\ Y_3 \end{bmatrix} \right)_{(q^n, r^n)}$$

Now, introduce the following notations.

$$\begin{aligned} \frac{\partial Y_1}{\partial q} &= Y_5, & \frac{\partial Y_2}{\partial q} &= Y_6, & \frac{\partial Y_3}{\partial q} &= Y_7, & \frac{\partial Y_4}{\partial q} &= Y_8, \\ \frac{\partial Y_1}{\partial r} &= Y_9, & \frac{\partial Y_2}{\partial r} &= Y_{10}, & \frac{\partial Y_3}{\partial r} &= Y_{11}, & \frac{\partial Y_4}{\partial r} &= Y_{12}. \end{aligned}$$

As a result of these new notations, the Newton's iterative scheme gets the following form.

$$\begin{bmatrix} q^{n+1} \\ r^{n+1} \end{bmatrix} = \begin{bmatrix} q^n \\ r^n \end{bmatrix} - \left(\begin{bmatrix} Y_5 & Y_9 \\ Y_7 & Y_{11} \end{bmatrix}^{-1} \begin{bmatrix} Y_1 \\ Y_3 \end{bmatrix} \right)_{(q^n, r^n)}.$$

Now differentiating the system of four first order ODEs with respect to q and r we get

$$\begin{aligned} Y_5' &= Y_6, & Y_5(0) &= B. \\ Y_6' &= - \left(P_r C_1 Y_6 + \frac{N_c}{Le} (Y_6 Y_4 + Y_2 Y_8) + \frac{2N_c}{Le N_{bt}} Y_2 Y_6 \right), & Y_6(0) &= 1, \\ Y_7' &= Y_8, & Y_7(0) &= 0. \\ Y_8' &= -S_c C_1 Y_8 + \frac{1}{N_{bt}} \left(P_r C_1 Y_6 + \frac{N_c}{Le} (Y_4 Y_6 + Y_2 Y_8) + \frac{2N_c}{Le N_{bt}} Y_2 Y_6 \right), & Y_4(0) &= 0. \\ Y_9' &= Y_{10}, & Y_9(0) &= 0. \\ Y_{10}' &= - \left(P_r C_1 Y_{10} + \frac{N_c}{Le} (Y_4 Y_{10} + Y_2 Y_{12}) + \frac{2N_c}{Le N_{bt}} Y_2 Y_{10} \right), & Y_{10}(0) &= 0. \\ Y_{11}' &= Y_{12}, & Y_{11}(0) &= 0. \\ Y_{12}' &= -S_c C_1 Y_{12} + \frac{1}{N_{bt}} \left(P_r C_1 Y_{10} + \frac{N_c}{Le} (Y_4 Y_{10} + Y_2 Y_{12}) + \frac{2N_c}{Le N_{bt}} Y_2 Y_{10} \right), & Y_{12}(0) &= 1. \end{aligned}$$

The stopping criteria for the Newton's method is set as

$$\max\{|Y_1(q, r)|, |Y_3(q, r)|\} < \epsilon.$$

3.4 Representation of Graphs and Tables

This section includes a thorough discussion on the numerical results in the form of graphs and tables. The main focus of this section will be on the physical impacts of significant parameters on skin friction, Nusslet number and Sherwood number.

The results presented in Table 3.1 demonstrate the impact of significant parameters on the skin friction coefficients $Re^{\frac{1}{2}} C_{fx}$. For the rising values of velocity slip parameter δ , the skin friction coefficient is increased. However, by increasing the

value of the Williamson parameter λ , the skin friction coefficient is dropped.

Table 3.2, illustrates the impact of significant parameters on Sherwood number $Re^{-\frac{1}{2}}Sh_x$. It is found that the values of Sherwood number $Re^{-\frac{1}{2}}Nu_x$ are dropped due to the accelerating values of the velocity slip parameter δ and Williamson parameter λ , while for the accelerating value of thermal slip parameter β , diffusivity ratio parameter Nbt and Schmidt number Sc , the Sherwood number is increased. Table 3.3 demonstrates the effects of some dimensionless parameters on Nusslet number $Re^{-\frac{1}{2}}Nu_x$. It can be found that by enhancing the values of the velocity slip parameter, thermal slip parameter, Williamson parameter and heat capacity ratio parameter, the value of Nusslet number $Re^{-\frac{1}{2}}Nu_x$ is dropped. Furthermore by increasing the value of the diffusivity parameter, Prandtl number and Lewis number, the value of Nusslet number $Re^{-\frac{1}{2}}Nu_x$ is increased.

Figures 3.2 and 3.3 show the impact of the velocity slip parameter and Williamson parameter on the velocity profile $f'(\eta)$. It is found that the velocity profile is decreasing as the velocity slip parameter and Williamson parameter enhance.

Figures 3.4, 3.6 and 3.8 describe the impact of the velocity slip parameter, Williamson parameter and heat capacity ratio parameter on temperature profile $\theta(\eta)$. Results show that by increasing the value of the above parameters, the value of temperature profile $\theta(\eta)$ is enhanced. It is found that the skin fraction coefficient for Williamson nanofluid is getting low as the Williamson parameter increases. It is very useful as lubricant in cooling system due to the reason that the suspended nanoparticles could keep longer in the sub-structural fluid and increase the flow characteristics of nanofluids.

Figures 3.5, 3.7, 3.9 and 3.10 indicate that by increasing the values of the diffusivity ratio parameter, Prandtl number, Lewis number and thermal slip parameter, the temperature profile $\theta(\eta)$ is declined. An increment in Prandtl number causes the slow rate in thermal diffusion. Physically, it means that fluid with high Prandtl number has large viscosity and small thermal conductivity, which implies that the fluid becomes thick which decreases the velocity of the fluid. Figure 3.11 and 3.13 describe the impact of the velocity slip parameter and Williamson parameter on the concentration profile $\phi(\eta)$. By increasing the value of the velocity slip parameter and Williamson slip parameter, the concentration profile $\phi(\eta)$ is enhanced.

Figures 3.12 and 3.14 describe the impact of diffusivity ratio parameter and thermal slip parameter on the concentration profile $\phi(\eta)$. Results indicate that by enhancing the value of diffusivity ratio parameter and thermal slip parameter concentration profile is decreased. Figure 3.15, shows the influence of Schmidt number on the concentration profile $\phi(\eta)$. By increasing Schmidt number, the value of the concentration profile $\phi(\eta)$ is dropped. This is because due to the momentum, diffusivity would increase and at the same time it will slow down the effects of the mass transfer rate leading to a reduction in the concentration profile.

TABLE 3.1: Impact of δ and λ on skin fraction

δ	λ	I_g	C_{fx}
0.25	0.5	[-0.8,0.8]	-0.824627
0.75		[-0.5,0.8]	-0.521313
1.25		[-0.4,0.8]	-0.391317
1.75		[-0.3,0.8]	-0.316124
0.5	0	[-0.5,0.8]	-0.430631
	0.2	[-0.5,0.8]	-0.442676
	0.8	[-0.5,0.8]	-0.457476
	1.4	[-0.6,0.8]	-0.489301

TABLE 3.2: Effects of various parameters on Sherwood Number

δ	β	λ	Nbt	I_q	I_r	Sh		
0.25	1	0.5	2	[-9.4,7]	[-9.1,7]	1.20844		
0.75				[-8.3,7]	[-8.0,7]	1.05352		
1.25				[-7.7,7]	[-7.3,7]	0.95993		
1.75				[-7.5,7]	[-6.4,7]	0.89353		
0.5	0.2	0	2	[-9.8,7]	[-6.0,7]	0.98078		
				0.4	[-9.8,7]	[-6.0,7]	1.03282	
				0.6	[-9.8,7]	[-6.0,7]	1.06981	
				0.8	[-9.8,7]	[-6.0,7]	1.09554	
	0.4	0.4	0.4	2	[-8.5,7]	[-4.0,7]	1.05297	
					0.8	[-8.3,7]	[-4.0,7]	1.03313
					0.8	[-8.0,7]	[-4.0,7]	1.00939
					1.4	[-7.7,7]	[-3.7,7]	0.96174
0.3	0.4	0.4	0.3	[-2.2,8]	[-1.6,8]	0.26600		
				0.4	[-2.9,8]	[-1.9,8]	0.50018	
				0.6	[-4.3,8]	[-2.1,8]	0.74850	
				0.9	[-5.5,8]	[-4.3,8]	0.92166	

TABLE 3.3: Effects of various parameters on Nusselt Number

δ	β	λ	Pr	Nc	Nbt	Le	I_q	I_r	Nu
0.25	1	0.5	7	2.5	2	[-9.4,7]	[-9.1,7]		0.59575
0.75						[-8.3,7]	[-8.0,7]		0.56428
1.25						[-7.7,7]	[-7.3,7]		0.54276
1.75						[-7.5,7]	[-6.4,7]		0.52612
	0.2					[-9.8,7]	[-6.0,7]		1.06418
	0.4					[-9.8,7]	[-6.0,7]		0.88039
	0.6					[-9.8,7]	[-6.0,7]		0.75008
	0.8					[-9.8,7]	[-6.0,7]		0.65308
		0				[-9.8,7]	[-6.0,7]		0.50583
		0.4				[-8.5,7]	[-4.0,7]		0.50151
		0.8				[-8.3,7]	[-4.0,7]		0.49620
		1.4				[-8.0,7]	[-4.0,7]		0.48505
			4			[-7.8,7]	[-4.0,7]		0.49037
			6			[-8.9,7]	[-6.6,7]		0.55456
			8			[-9.5,7]	[-9.2,7]		0.59807
			10			[-11,7]	[-9.8,7]		0.63027
				5		[-6.2,7]	[-2.0,7]		0.54461
				10		[-3.0,8]	[-1.0,8]		0.47062
				15		[-1.8,8]	[-1.0,8]		0.38967
				20		[-1.4,8]	[-0.6,8]		0.30735
					0.3	[-2.2,8]	[-1.6,8]		0.55491
					0.4	[-2.9,8]	[-1.9,8]		0.56202
					0.6	[-4.3,8]	[-2.1,8]		0.56889
					0.9	[-5.5,8]	[-4.3,8]		0.57335

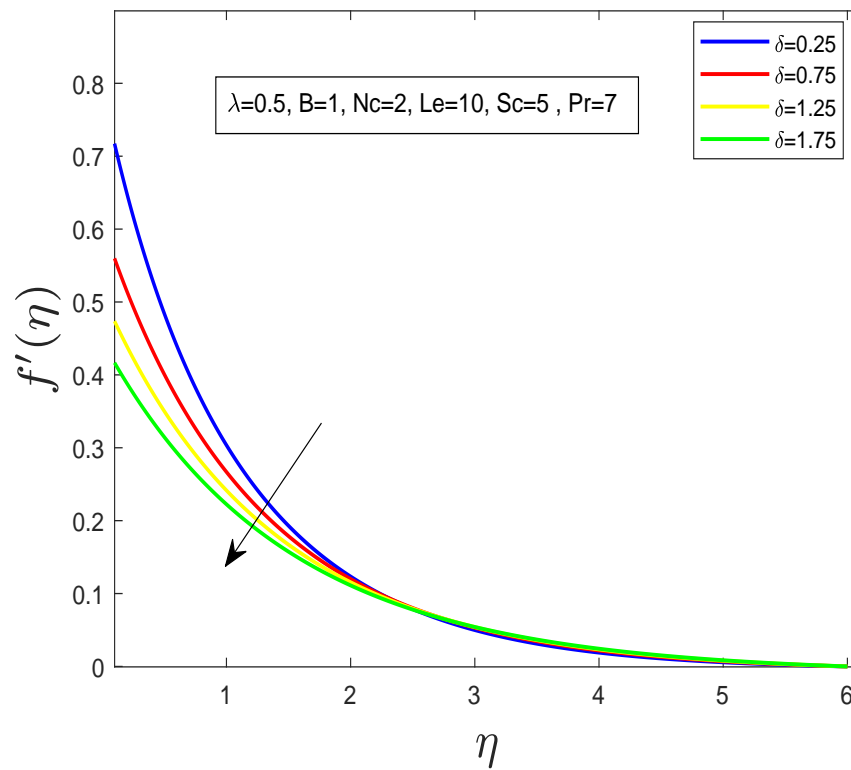


FIGURE 3.2: Change in $f'(\eta)$ for rising value of δ .

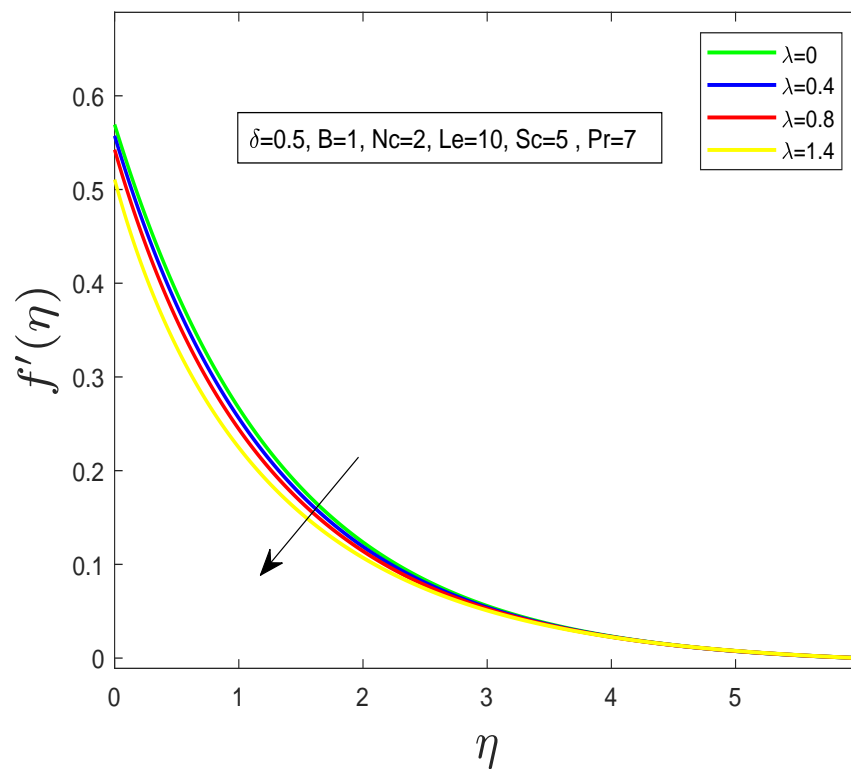


FIGURE 3.3: Change in $f'(\eta)$ for rising value of λ .

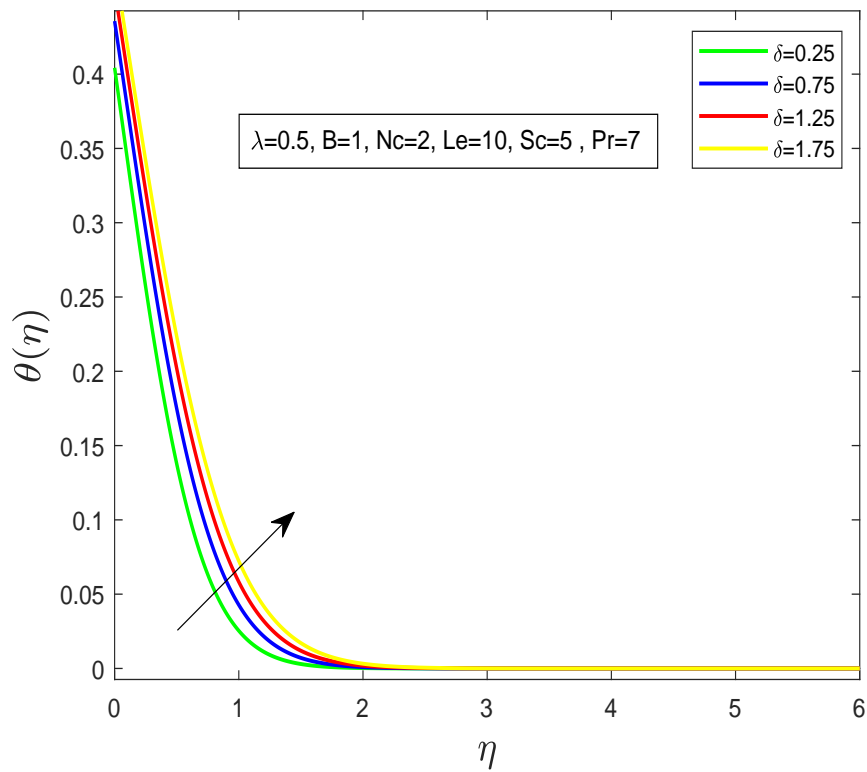


FIGURE 3.4: Change in $\theta(\eta)$ for rising value of δ .

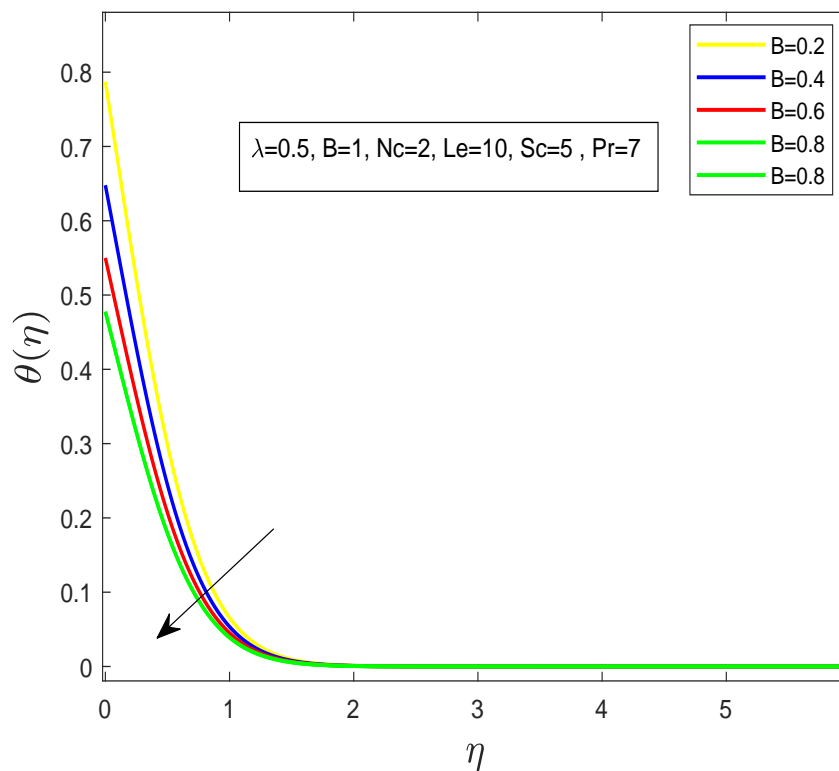


FIGURE 3.5: Change in $\theta(\eta)$ for rising value of B .

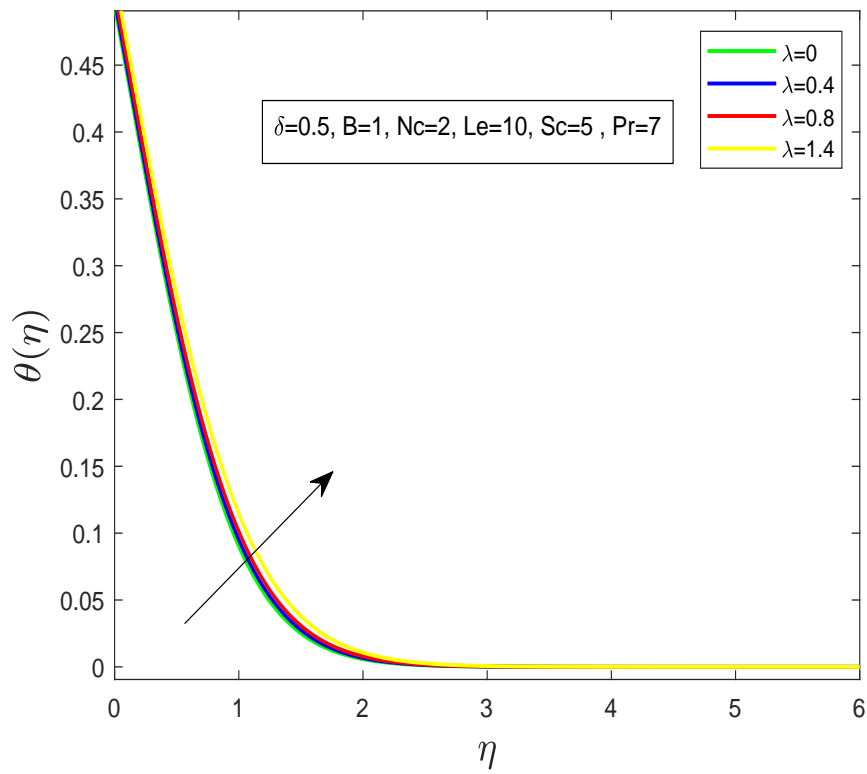


FIGURE 3.6: Change in $\theta(\eta)$ for rising value of λ .

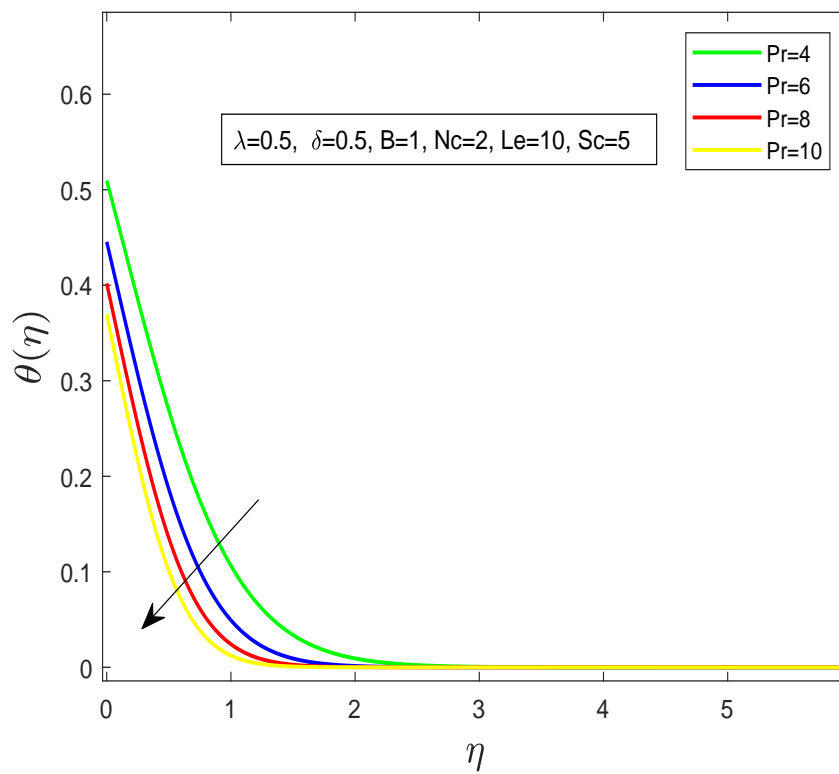


FIGURE 3.7: Change in $\theta(\eta)$ for rising value of Pr .

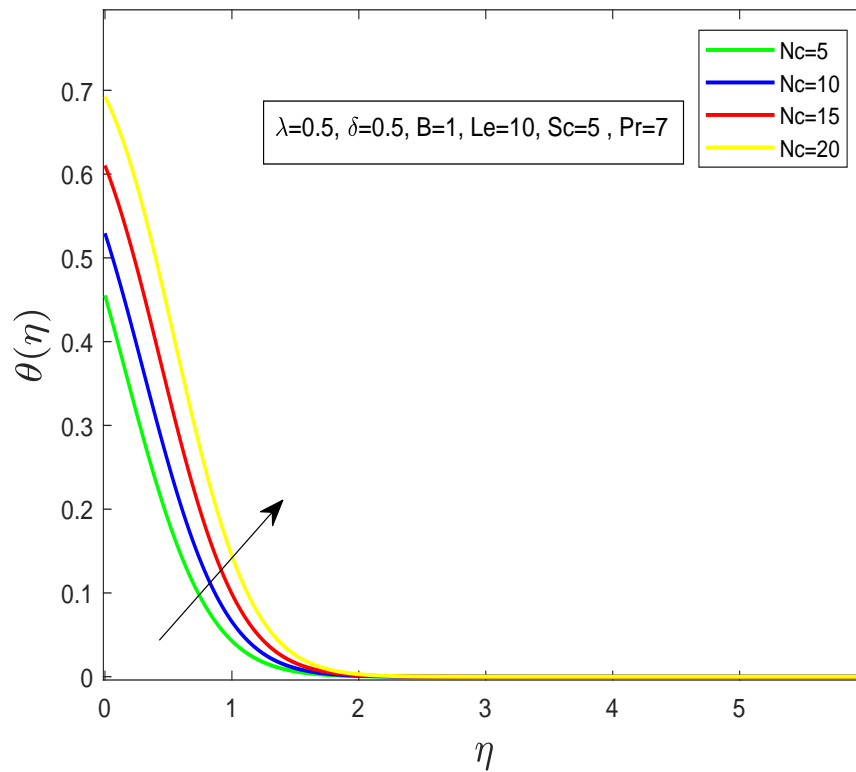


FIGURE 3.8: Change in $\theta(\eta)$ for rising value of N_c .

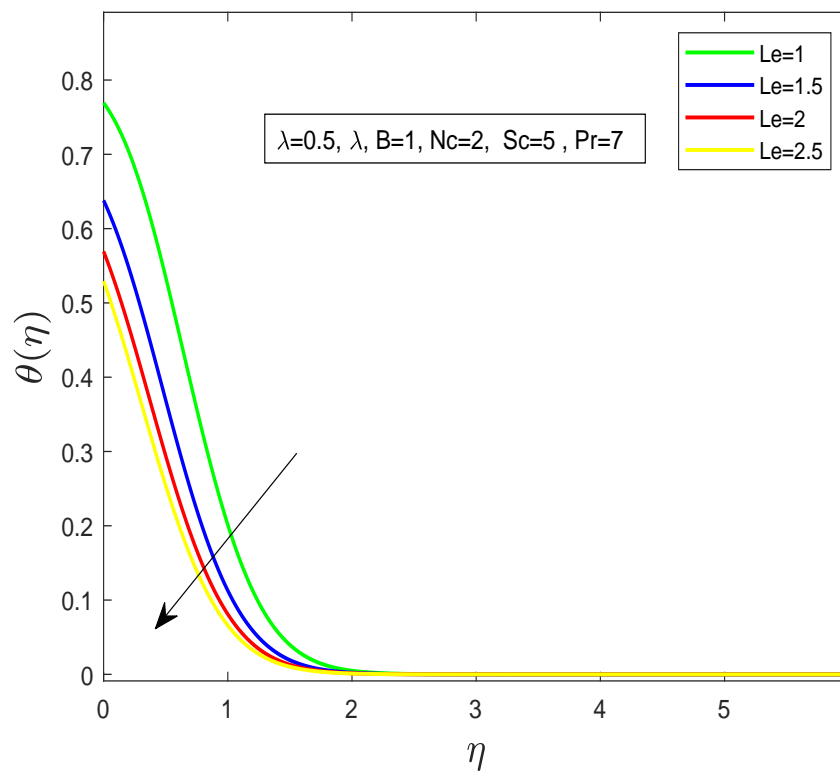


FIGURE 3.9: Change in $\theta(\eta)$ for rising value of Le .

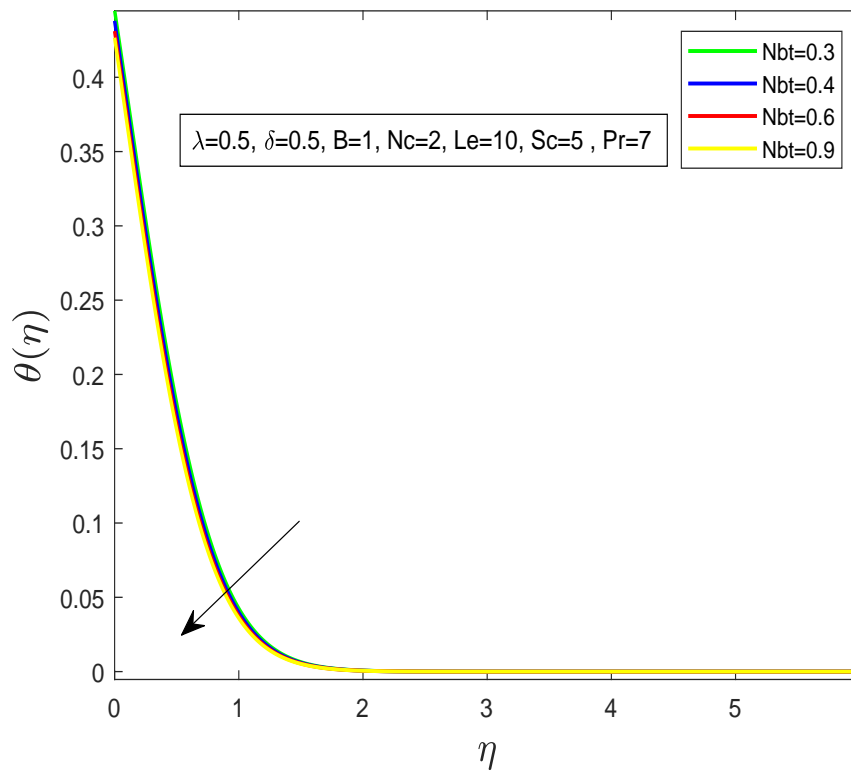


FIGURE 3.10: Change in $\theta(\eta)$ for rising value of Nbt .

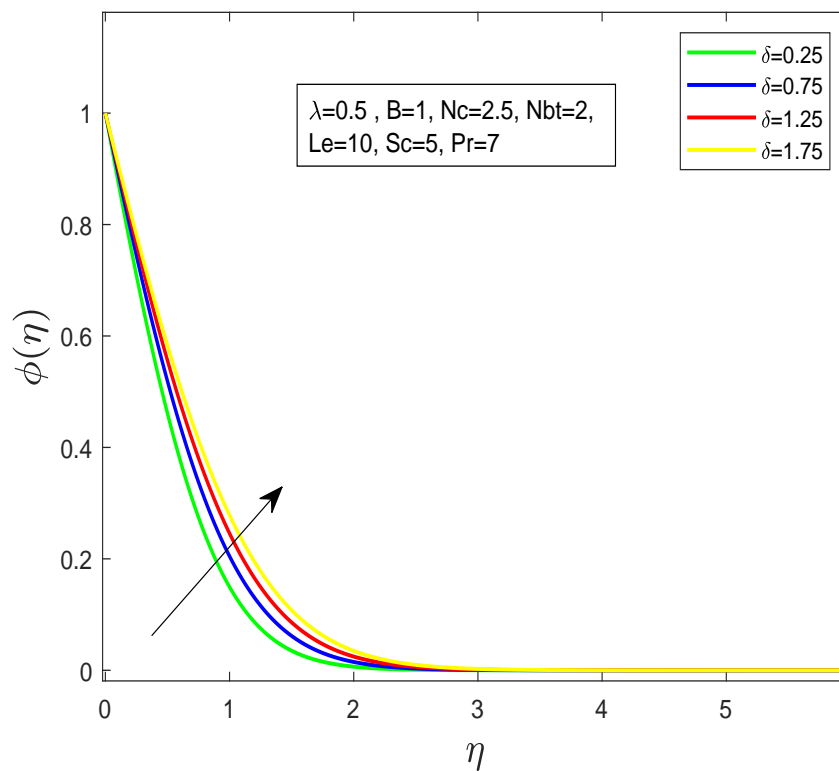


FIGURE 3.11: Change in $\phi(\eta)$ for rising value of δ .

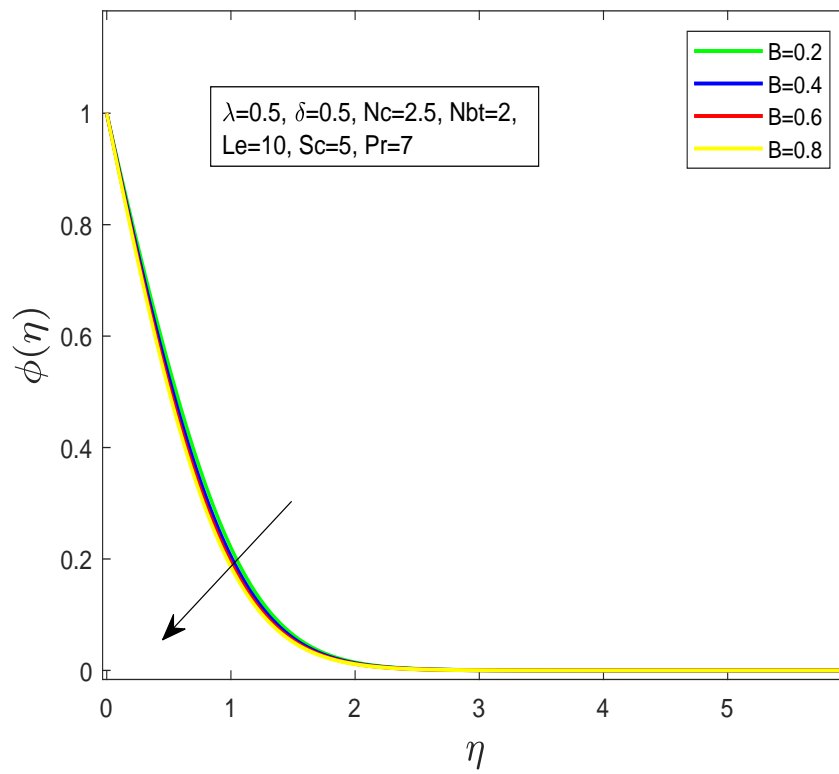


FIGURE 3.12: Change in $\phi(\eta)$ for rising value of B .

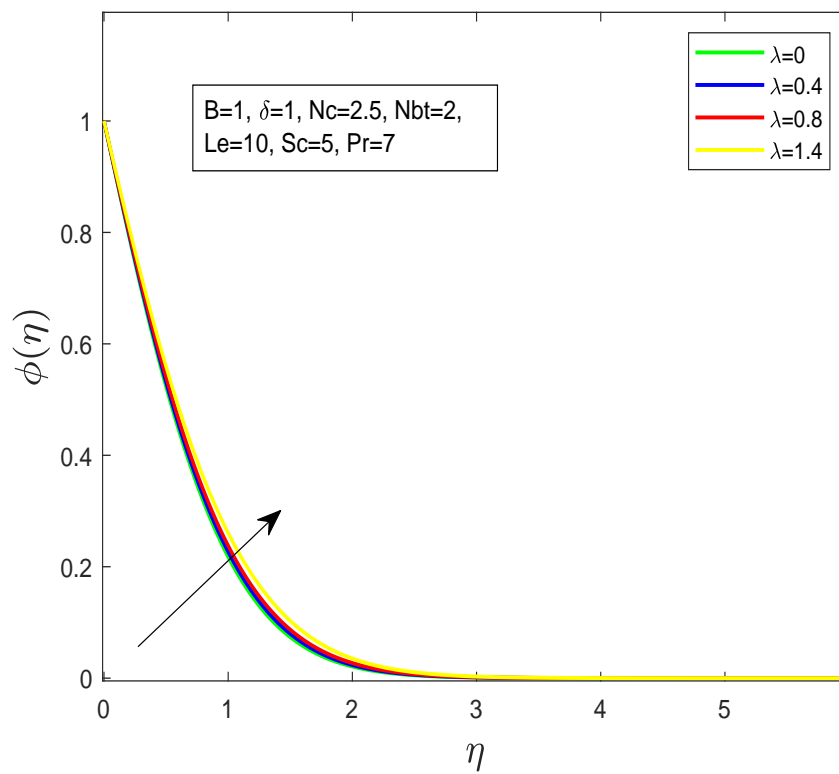


FIGURE 3.13: Change in $\phi(\eta)$ for rising value of λ .

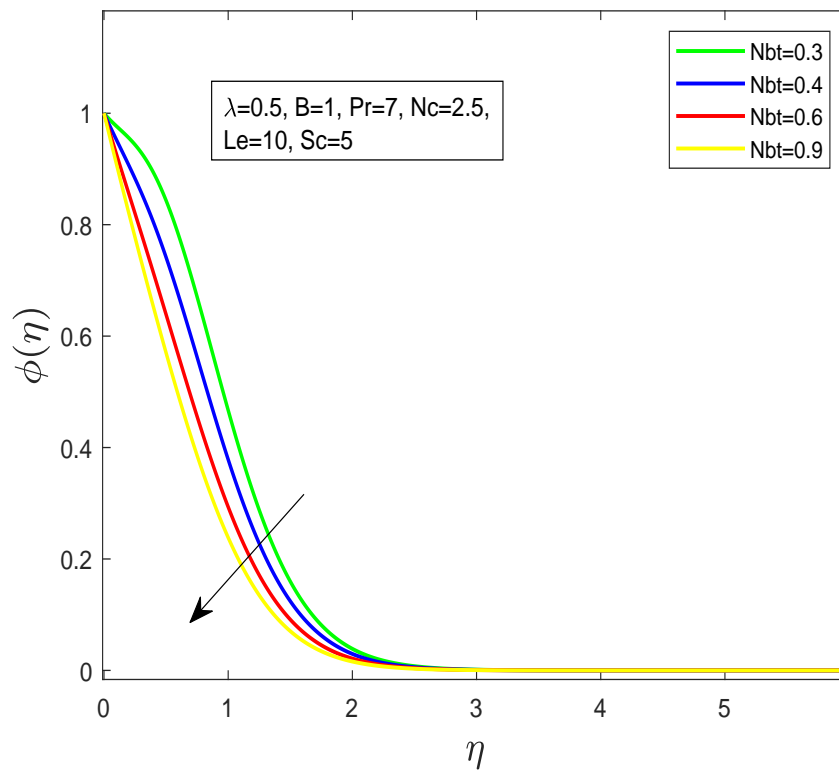


FIGURE 3.14: Change in $\phi(\eta)$ for rising value of Nbt .

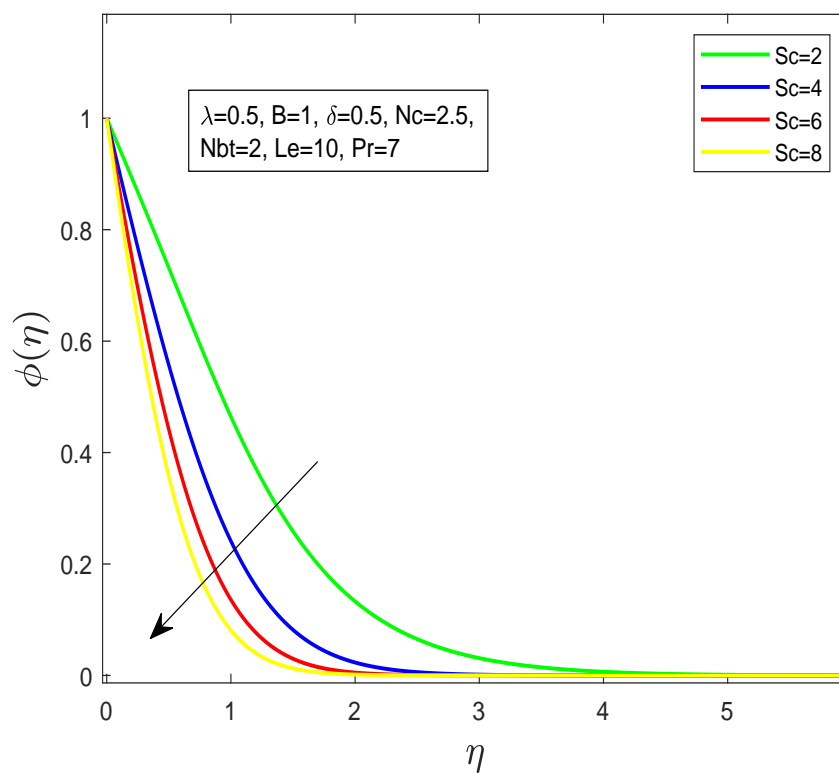


FIGURE 3.15: Change in $\phi(\eta)$ for rising value of Sc .

Chapter 4

Williamson Nanofluid flow with MHD, Porosity, Joule Heating and Activation Energy.

4.1 Introduction

This chapter demonstrates the extension of the model discussed in Chapter 3 by adding MHD and porous parameter in the momentum equation. The behavior of temperature and concentration profiles is further analyzed by including Joule heating and activation energy respectively. Furthermore, by using the similarity transformations, the nonlinear PDEs are transformed into a system of ODEs. By using the shooting method, the numerical solution of ODEs is obtained. At the end of this chapter, the final concluding results are illustrated for some significant parameters that have impact on the velocity, temperature and concentration profiles. For a quantitative view, the obtained findings are expressed in tables and graphs.

4.2 Mathematical Modeling

Consider a steady, incompressible flow of non-Newtonian Williamson nanofluid past over a stretching sheet in porous medium. The linear stretching velocity

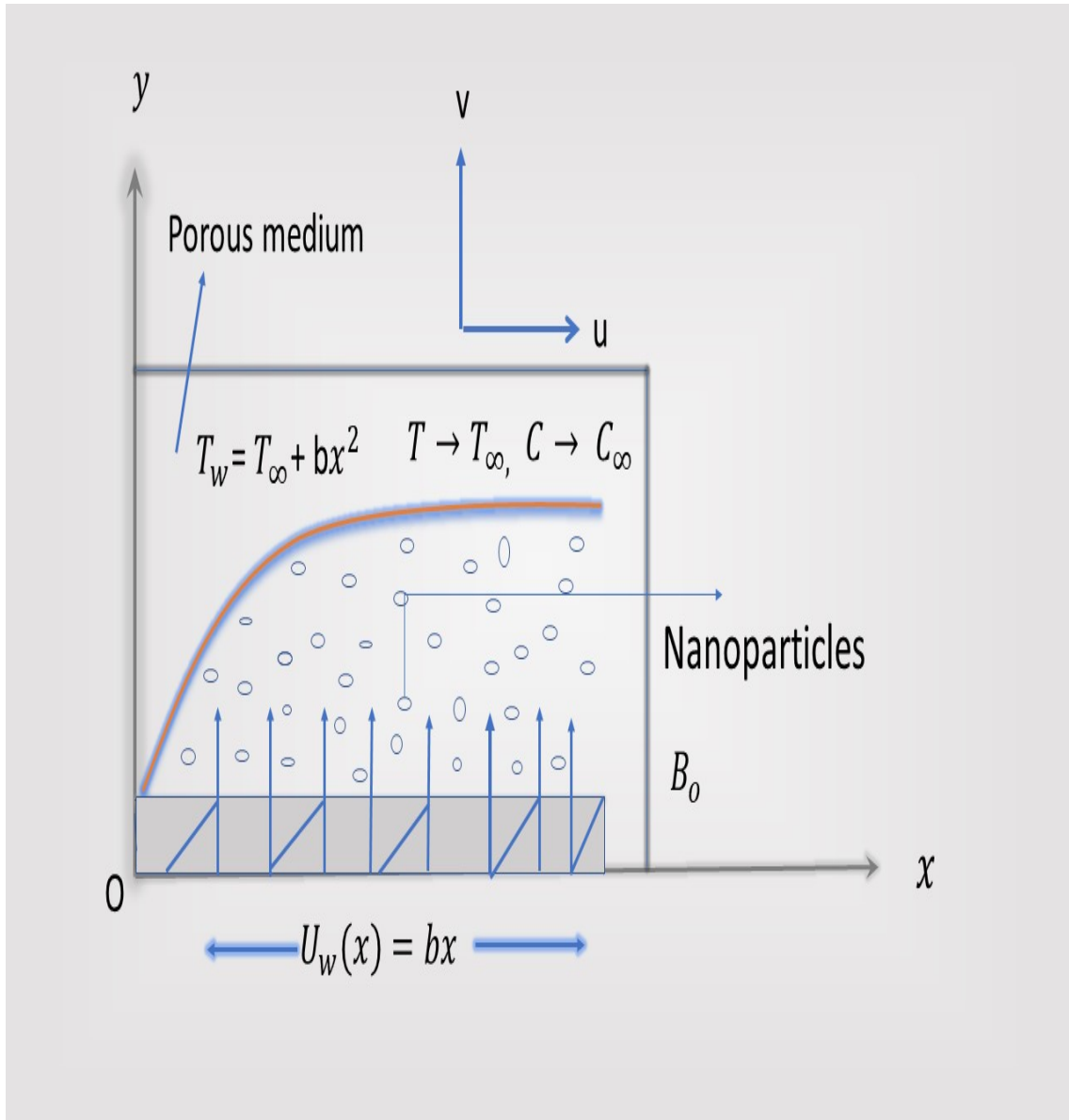


FIGURE 4.1: Geometric representation of the physical model.

of the sheet has been taken as $U_w(x) = bx$, where b is a constant and x is the coordinate measure along the stretching sheet respectively. The y -axis has been taken perpendicular to the stretching sheet. An external magnetic field B_0 is applied along y -axis. In the presence of the Joule heating and activation energy, energy transport and concentration of fluid flow is analyzed respectively. The wall temperature has been taken taken as $T_w = T_\infty + bx^2$ where T_∞ is the ambient temperature. The fluid concentration at the sheet C_w is considered as constant throughout the stretching surface and when y continuously approaches to infinity, approach to C_∞ .

Associated governing equations can be expressed as

$$\frac{\partial u}{\partial x} + \frac{\partial v}{\partial y} = 0, \quad (4.1)$$

$$u \frac{\partial u}{\partial x} + v \frac{\partial u}{\partial y} = \nu \frac{\partial^2 u}{\partial y^2} + \sqrt{2\nu}\Gamma \frac{\partial u}{\partial y} \frac{\partial^2 u}{\partial y^2} - \alpha \frac{B_0^2 u}{\rho} - \frac{\nu u}{k_p^*}, \quad (4.2)$$

$$u \frac{\partial T}{\partial x} + v \frac{\partial T}{\partial y} = \alpha \left(\frac{\partial^2 T}{\partial y^2} \right) + \frac{\rho_p C_p}{\rho C} \left[D_B \frac{\partial C}{\partial y} \frac{\partial T}{\partial y} + \frac{D_T}{T_\infty} \left(\frac{\partial T}{\partial y} \right)^2 \right] + \frac{\alpha B_0^2 u^2}{\rho C_p}, \quad (4.3)$$

$$u \frac{\partial C}{\partial x} + v \frac{\partial C}{\partial y} = D_B \frac{\partial^2 C}{\partial y^2} + \frac{D_T}{T_\infty} \frac{\partial^2 T}{\partial y^2} + k_0^2 (C - C_\infty) \left(\frac{T}{T_\infty} \right)^n \exp \left[\frac{-Ea}{kT} \right]. \quad (4.4)$$

The associated BCs have been taken as

$$\left. \begin{aligned} u &= u_w + \delta^* \mu \left(\frac{\partial u}{\partial y} \right), \quad v = 0, \quad T = T_w + B * \frac{\partial T}{\partial y}, \quad C = C_w, \quad \text{at } y = 0, \\ u &\rightarrow 0, \quad T \rightarrow T_\infty, \quad C = C_\infty, \quad \text{as } y \rightarrow \infty. \end{aligned} \right\} \quad (4.5)$$

For the conversion of the mathematical model (4.1)-(4.4) into the ODEs, the following similarity transformation will be used.

$$\left. \begin{aligned} u &= bx f'(\eta), \quad v = -(b\nu)^{\frac{1}{2}} f(\eta), \quad \eta = \sqrt{\frac{b}{\nu}} y, \\ \theta(\eta) &= \frac{T - T_\infty}{T_w - T_\infty}, \quad \phi(\eta) = \frac{C - C_\infty}{C_w - C_\infty}. \end{aligned} \right\} \quad (4.6)$$

Equation (4.1) can easily satisfied same as (3.1) in Chapter 3.

For the conversion of momentum equation (4.2) into the dimensionless form, we will use following derivatives and the rest of them from Chapter 3

$$\frac{\alpha B_0^2 u}{\rho} = \frac{\alpha B_0^2}{\rho} bx f'(\eta). \quad (4.7)$$

$$\frac{\nu u}{k_p^*} = \frac{\nu bx f'(\eta)}{k_p^*}. \quad (4.8)$$

The left hand side of (4.2) is the same as that (3.2) in Chapter 3 i.e

$$u \frac{\partial u}{\partial x} + v \frac{\partial u}{\partial y} = b^2 x f'^2(\eta) - b^2 x f(\eta) f''(\eta). \quad (4.9)$$

Using (4.7), (4.8) and the rest of derivatives from Chapter 3, in the right side of equation (4.2), we get

$$\begin{aligned} \nu \frac{\partial^2 u}{\partial y^2} + \sqrt{2\nu\Gamma} \frac{\partial u}{\partial y} \frac{\partial^2 u}{\partial y^2} - \frac{\alpha B_0^2 u}{\rho} - \frac{\nu u}{k_p^*} = \\ b^2 x f'''(\eta) + \sqrt{2\nu\Gamma} b x^2 \sqrt{\frac{b^3}{\nu}} f''(\eta) f'''(\eta) - \frac{\alpha B_0^2}{\rho} b x f'(\eta) - \frac{\nu b x f'(\eta)}{k_p^*}. \end{aligned} \quad (4.10)$$

By comparing (4.9) and (4.10), the dimensionless form of (4.2) can be written as

$$\begin{aligned} b^2 x f'^2(\eta) - b^2 x f(\eta) f''(\eta) &= b^2 x f'''(\eta) + \sqrt{2\nu\Gamma} b x^2 \sqrt{\frac{b^3}{\nu}} f''(\eta) f'''(\eta) \\ &\quad - \frac{\alpha B_0^2}{\rho} b x f'(\eta) - \frac{\nu b x f'(\eta)}{k_p^*}, \\ \Rightarrow b^2 x (f'^2(\eta) - f(\eta) f''(\eta)) &= \\ &\quad b^2 x \left(f'''(\eta) + \sqrt{2\nu\Gamma} \sqrt{\frac{b^3}{\nu}} f''(\eta) f'''(\eta) - \frac{\alpha B_0^2}{b\rho} f'(\eta) - \frac{\nu f'(\eta)}{b k_p^*} \right). \\ \Rightarrow f'^2(\eta) - f(\eta) f''(\eta) &= f'''(\eta) + \sqrt{2\nu\Gamma} \sqrt{\frac{b^3}{\nu}} f''(\eta) f'''(\eta) - \frac{\alpha B_0^2}{b\rho} f'(\eta) - \frac{\nu f'(\eta)}{b k_p^*}. \\ \Rightarrow f'''(\eta) + \sqrt{2\nu\Gamma} \sqrt{\frac{b^3}{\nu}} f''(\eta) f'''(\eta) &+ f(\eta) f''(\eta) - f'^2(\eta) \\ &\quad - \left(\frac{\alpha B_0^2}{b\rho} + \frac{\nu}{b k_p^*} \right) f'(\eta) = 0. \\ \Rightarrow f'''(\eta) + \lambda f''(\eta) f'''(\eta) + f(\eta) f''(\eta) &- f'^2(\eta) - (k_1 + M_n) f'(\eta) = 0. \end{aligned} \quad (4.11)$$

For the conversion of equation (4.3) into the dimensionless form, we will use the following derivatives and the rest of them from Chapter 3, we get

$$\frac{\alpha B_0^2 u^2}{\rho C_P} = \frac{\alpha B_0^2}{\rho C_P} b^2 x^2 f'^2. \quad (4.12)$$

The left hand side of (4.3) is same as that (3.3) in Chapter 3 i.e

$$\Rightarrow u \frac{\partial T}{\partial x} + v \frac{\partial T}{\partial y} = -b(T_w - T_\infty) f(\eta) \theta'(\eta). \quad (4.13)$$

Now, using equations (4.12) and the rest of derivatives from Chapter 3, in right side of equation (4.3), to get

$$\alpha \left(\frac{\partial^2 T}{\partial y^2} \right) + \frac{\rho_p C_p}{\rho C} \left[D_B \frac{\partial C}{\partial y} \frac{\partial T}{\partial y} + \frac{D_T}{T_\infty} \left(\frac{\partial T}{\partial y} \right)^2 \right] + \frac{\alpha B_0^2 u^2}{\rho C_P} =$$

$$\begin{aligned} & \alpha \frac{b}{\nu} (T_w - T_\infty) \theta''(\eta) + \frac{\rho_p C_p}{\rho C} D_B (T_w - T_\infty) (C_w - C_\infty) \theta'(\eta) \phi'(\eta) \frac{b}{\nu} \\ & + \frac{\rho_p C_p}{\rho C} \frac{D_T}{T_\infty} \left(\frac{b}{\nu} (T_w - T_\infty)^2 \theta'^2(\eta) \right) + \frac{\alpha B_0^2}{\rho C_P} b^2 x^2 f'^2. \end{aligned} \quad (4.14)$$

By comparing equation (4.13) and (4.14), we can obtain the dimensionless form of equation (4.3), which is as below

$$\begin{aligned} & -b(T_w - T_\infty) f(\eta) \theta'(\eta) = \\ & \alpha \frac{b}{\nu} (T_w - T_\infty) \theta''(\eta) + \frac{\rho_p C_p}{\rho C} D_B (T_w - T_\infty) (C_w - C_\infty) \theta'(\eta) \phi'(\eta) \frac{b}{\nu} \\ & + \frac{\rho_p C_p}{\rho C} \frac{D_T}{T_\infty} \left(\frac{b}{\nu} (T_w - T_\infty)^2 \theta'^2(\eta) \right) + \frac{\alpha B_0^2}{\rho C_P} b^2 x^2 f'^2. \\ \Rightarrow & \alpha \frac{b}{\nu} (T_w - T_\infty) \theta''(\eta) + \frac{\rho_p C_p}{\rho C} D_B (T_w - T_\infty) (C_w - C_\infty) \theta'(\eta) \phi'(\eta) \frac{b}{\nu} \\ & + \frac{\rho_p C_p}{\rho C} \frac{D_T}{T_\infty} \left(\frac{b}{\nu} (T_w - T_\infty)^2 \theta'^2(\eta) \right) + b(T_w - T_\infty) f(\eta) \theta'(\eta) \\ & + \frac{\alpha B_0^2}{\rho C_P} b^2 x^2 f'^2 = 0. \\ \Rightarrow & \alpha \frac{b}{\nu} (T_w - T_\infty) \left(\theta''(\eta) + \frac{\nu}{\alpha} f(\eta) \theta'(\eta) + \frac{\rho_p C_p}{\rho C} \frac{D_B}{\alpha} (C_w - C_\infty) \theta'(\eta) \phi'(\eta) \right) + \\ & \alpha \frac{b}{\nu} (T_w - T_\infty) \left(\frac{\rho_p C_p}{\rho C} \frac{D_T}{T_\infty} (T_w - T_\infty) \theta'^2(\eta) + \frac{\sigma \nu B_0^2}{\rho C_P \alpha (T_w - T_\infty)} b x^2 f'^2 \right) = 0. \\ \Rightarrow & \theta''(\eta) + \frac{\nu}{\alpha} f(\eta) \theta'(\eta) + \frac{\rho_p C_p}{\rho C} \frac{D_B}{\alpha} (C_w - C_\infty) \theta'(\eta) \phi'(\eta) \\ & + \frac{\rho_p C_p}{\rho C} \frac{D_T}{T_\infty} (T_w - T_\infty) \theta'^2(\eta) = 0. \\ \Rightarrow & \theta''(\eta) + Pr f(\eta) \theta'(\eta) + \frac{Nc}{Le} \theta'(\eta) \phi'(\eta) + \frac{Nc}{Le Nbt} \theta'^2(\eta) \\ & + Pr ME_c f'^2 = 0. \end{aligned} \quad (4.15)$$

For the conversion of equation (4.4) into the dimensionless form, we will use the following derivatives and the rest of them from Chapter 3, we get

- $$\begin{aligned} \left(\frac{T}{T_\infty} \right)^n &= \left(\frac{\theta(T_w - T_\infty) + T_\infty}{T_\infty} \right)^n \\ &= \left(\theta \frac{T_w - T_\infty}{T_\infty} + 1 \right)^n \\ &= (\theta \delta^* + 1)^n \end{aligned} \quad (4.16)$$
- $$\exp\left(-\frac{Ea}{kT}\right) = \exp\left(-\frac{Ea}{k(\theta(T_w - T_\infty) + T_\infty)}\right)$$

$$\begin{aligned}
&= \exp\left(-\frac{Ea}{k\left(\frac{\theta(T_w-T_\infty)+T_\infty}{T_\infty}\right)T_\infty}\right) \\
&= \exp\left(-\frac{Ea}{k\left(\frac{\theta(T_w-T_\infty)+T_\infty}{T_\infty}\right)T_\infty}\right) \\
&= \exp\left(-\frac{Ea}{k\left(\theta\frac{T_w-T_\infty}{T_\infty}+1\right)T_\infty}\right) \\
&= \exp\left(-\frac{Ea}{k(\theta\delta^*+1)T_\infty}\right). \tag{4.17}
\end{aligned}$$

$$\begin{aligned}
\bullet \quad C - C_\infty &= (\phi(C_w - C_\infty) + C_\infty) - C_\infty \\
&= \phi(C_w - C_\infty). \tag{4.18}
\end{aligned}$$

The left hand side of (4.4) is the same as that (3.4) in Chapter 3 i.e

$$u\frac{\partial C}{\partial y} + v\frac{\partial C}{\partial y} = -b(C_w - C_\infty)f(\eta)\phi'(\eta) \tag{4.19}$$

Now, using equation (4.16), (4.17), (4.18) and recall some derivatives from Chapter 3 in the right hand side of equation (4.4), we get

$$\begin{aligned}
D_B\frac{\partial^2 C}{\partial y^2} + \frac{D_T}{T_\infty}\frac{\partial^2 T}{\partial y^2} + k_0^2(C - C_\infty)\left(\frac{T}{T_\infty}\right)^n \exp\left[-\frac{Ea}{kT}\right] = \\
D_B\frac{b}{\nu}(C_w - C_\infty)\phi''(\eta) + \frac{D_T}{T_\infty}\frac{b}{\nu}(T_w - T_\infty)\theta''(\eta) \\
+ k_0^2(C_w - C_\infty)(\theta\delta^* + 1)^n \exp\left[\frac{-Ea}{(k\theta\delta^* + 1)T_\infty}\right]\phi. \tag{4.20}
\end{aligned}$$

By comparing equation (4.19) and (4.20), we can obtain the dimensionless form of equation (4.4), which is

$$\begin{aligned}
-b(C_w - C_\infty)f(\eta)\phi'(\eta) &= D_B\frac{b}{\nu}(C_w - C_\infty)\phi''(\eta) + \frac{D_T}{T_\infty}\frac{b}{\nu}(T_w - T_\infty)\theta''(\eta) \\
&\quad + k_0^2(C_w - C_\infty)(\theta\delta^* + 1)^n \exp\left[-\frac{Ea}{(\theta\delta^* + 1)kT_\infty}\right]\phi, \\
\Rightarrow D_B\frac{b}{\nu}(C_w - C_\infty)\phi''(\eta) + \frac{D_T}{T_\infty}\frac{b}{\nu}(T_w - T_\infty)\theta''(\eta) + b(C_w - C_\infty)f(\eta)\phi'(\eta) \\
&\quad + k_0^2(C_w - C_\infty)(\theta\delta^* + 1)^n \exp\left[-\frac{Ea}{(\theta\delta^* + 1)kT_\infty}\right]\phi = 0. \\
\Rightarrow D_B\frac{b}{\nu}(C_w - C_\infty)\left(\phi''(\eta) + \frac{D_T(T_w - T_\infty)}{D_B T_\infty(C_w - C_\infty)}\theta''(\eta) + \frac{\nu}{D_B}f(\eta)\phi'(\eta)\right)
\end{aligned}$$

$$\begin{aligned}
& + \frac{D_B b}{\nu} (C_w - C_\infty) \left[k_0^2 \frac{\nu}{b D_B} (\theta \delta^* + 1)^n \exp \left(-\frac{Ea}{(\theta \delta^* + 1) k T_\infty} \right) \right] \phi = 0. \\
\Rightarrow \quad & \phi''(\eta) + \frac{D_T (T_w - T_\infty)}{D_B T_\infty (C_w - C_\infty)} \theta''(\eta) + \frac{\nu}{D_B} f(\eta) \phi'(\eta) \\
& + k_0^2 \frac{\nu}{b D_B} (\theta \delta^* + 1)^n \exp \left(\frac{-Ea}{(\theta \delta^* + 1) k T_\infty} \right) \phi = 0. \\
\Rightarrow \quad & \phi''(\eta) + \frac{1}{Nbt} \theta''(\eta) + Sc f(\eta) \phi'(\eta) + S_c \sigma (1 + \delta^* \theta)^n \exp \left(-\frac{E1}{(1 + \delta^* \theta)} \right) \phi = 0.
\end{aligned} \tag{4.21}$$

The final dimensionless form of the model is

$$f'''(\eta) + \lambda f''(\eta) f'''(\eta) + f(\eta) f''(\eta) - f'^2(\eta) - (k_1 + M_n) f'(\eta) = 0. \tag{4.22}$$

$$\theta''(\eta) + Pr f(\eta) \theta'(\eta) + \frac{Nc}{Le} \theta'(\eta) \phi'(\eta) + \frac{Nc}{Le Nbt} \theta'^2(\eta) + Pr M E_c f'^2 = 0. \tag{4.23}$$

$$\begin{aligned}
& \phi''(\eta) + \frac{1}{Nbt} \theta''(\eta) + Sc f(\eta) \phi'(\eta) + \\
& S_c \sigma (1 + \delta^* \theta)^n \exp \left(\frac{-E1}{(1 + \delta^* \theta)} \right) \phi = 0.
\end{aligned} \tag{4.24}$$

The associated BCs (4.5) is same as that (3.5) in Chapter 3, i.e

$$\left. \begin{aligned}
& f(\eta) = 0, \quad f'(\eta) = 1 + \delta f''(\eta), \quad \theta(\eta) = 1 + \beta \theta'(\eta), \quad \phi(\eta) = 1 \quad \text{at } \eta = 0, \\
& f'(\eta) = 0, \quad \theta(\eta) = 0, \quad \phi(\eta) = 0 \quad \text{as } y \rightarrow \infty.
\end{aligned} \right\} \tag{4.25}$$

Here

$$M = \frac{\sigma B_0^2}{\alpha \rho}, \quad E_c = \frac{bx^2}{C_p (T_w - T_\infty)}, \quad \delta^* = \frac{T_w - T_\infty}{T_\infty}, \quad E_1 = \frac{E_a}{k T_\infty}, \quad \sigma = \frac{k_0^2}{b},$$

$$\beta = B^* \sqrt{\frac{b}{\nu}}, \quad \beta = B^* \sqrt{\frac{b}{\nu}}, \quad \delta = \delta^* \mu \sqrt{\frac{b}{\nu}}.$$

4.3 Numerical Method for Solution

The shooting method has been used to solve the ordinary differential equations (4.22). The following notations have been considered

$$f = Z_1, \quad f' = Z_1' = Z_2, \quad f'' = Z_1'' = Z_2' = Z_3, \quad f''' = Z_3'.$$

By applying following notations, equation (4.22) is converted into first order ODEs

$$\begin{aligned} Z_1' &= Z_2, & Z_1(0) &= 0. \\ Z_2' &= Z_3, & Z_2(0) &= 1 + \delta Z_3. \\ Z_3' &= \frac{1}{1 + \lambda Z_3} [(Z_2^2 - Z_3 Z_1) + (k_1 + M_n) Z_2]. & Z_3(0) &= m. \end{aligned}$$

The above initial value problem (IVP) will be numerically solved by the RK-4 method. For the numerical solution, the unbounded domain $[0, \infty [$ has been replaced by $[0, \eta_\infty]$ where η_∞ is a real number having the property that for $\eta > \eta_\infty$, there is no significant variation in the solution. In this initial value problem, the missing condition m is to be chosen such that

$$Z_2(\eta_\infty, m) = 0.$$

For the convenience, let us denote $Z_2(\eta_\infty, m) = 0$ by $Z_2(m)$. Such notations will also be used for all Z_i or their derivatives, where $i=1,2,\dots,6$. To find m we will use Newton's method which has the following iterative scheme,

$$m^{n+1} = m^n - \frac{Z_2(m^n)}{\left(\frac{\partial Z_2}{\partial m}\right)_{m=m^n}}$$

We further introduce, the following notations to obtain the derivative

$$\begin{aligned} \frac{\partial Z_1}{\partial m} &= Z_4, & \frac{\partial Z_2}{\partial m} &= Z_5, & \frac{\partial Z_3}{\partial m} &= Z_6. \\ Z_4' &= Z_5, & Z_4(0) &= 0. \\ Z_5' &= Z_6, & Z_5(0) &= 0. \\ Z_6' &= \frac{2Z_5 Z_2 - Z_1 Z_6 - Z_3 Z_6 + 2\lambda Z_2 Z_3 Z_5 - \lambda Z_3^2 Z_4 - \lambda Z_2^2 Z_6 + \lambda(k_1 + M_n) Z_2 Z_6}{(1 + \lambda Z_3)^2} \\ & & Z_6(0) &= 1. \end{aligned}$$

The stopping criteria for the Newton's technique is set as

$$| Z_2(m) | < \epsilon,$$

where $\epsilon > 0$ is an arbitrarily small positive number. From now onward ϵ has been taken as 10^{-10} .

The equation (4.23) and equation (4.24) are coupled equations will be solved numerically by using the shooting method by assuming f as a known function. For this we use the following notions

$$\theta = Y_1, \quad \theta' = Y_2, \quad \theta'' = Y_2'.$$

$$\phi = Y_3, \quad \phi' = Y_4, \quad \phi'' = Y_4'.$$

Now, we can write equations (4.23) and (4.24), in the form of first order ODEs.

$$\begin{aligned} Y_1' &= Y_2, & Y_1(0) &= 1 + Bu, \\ Y_2' &= - \left[P_r C_1 Y_2 + \frac{Nc}{Le} Y_2 Y_4 + \frac{Nc}{Le N_{bt}} Y_2^2 + P_r M E_c C_2 \right], & Y_2(0) &= u, \\ Y_3' &= Y_4, & Y_3(0) &= 1, \\ Y_4' &= - \left[Sc C_1 Y_4 + \frac{1}{N_{bt}} \left(- (P_r C_1 Y_2 + \frac{Nc}{Le} Y_2 Y_4 + \frac{Nc}{Le N_{bt}} Y_2^2) \right) \right. \\ &\quad \left. - \left[Sc \sigma (1 + \delta^* \theta)^n \exp \left(\frac{-E1}{1 + \delta^* \theta} \right) Y_3 \right] \right], & Y_4(0) &= v, \\ Y_4' &= - \left[Sc C_1 Y_4 - \frac{1}{N_{bt}} \left(P_r C_1 Y_2 + \frac{Nc}{Le} Y_2 Y_4 + \frac{Nc}{Le N_{bt}} Y_2^2 \right) \right. \\ &\quad \left. - \left[Sc \sigma (1 + \delta^* \theta)^n \exp \left(\frac{-E1}{1 + \delta^* \theta} \right) Y_3 \right] \right], & Y_4(0) &= v. \end{aligned}$$

The RK-4 method has been taken into consideration for solving the above initial value problem. For the above system of equations, the missing conditions are to be chosen such that

$$(Y_1(u, v)) = 0, \quad (Y_3(u, v)) = 0.$$

Note that $Y_i(u, v)$ and their partial derivatives w.r.t u and v at $\eta = \eta_\infty$ will be denoted by $Y_i(u, v)$, $\frac{\partial Y_i}{\partial u}$, and $\frac{\partial Y_i}{\partial v}$, where $i = 1, 2, 3, \dots, 12$.

To solve the above algebraic equations, we apply the Newton's method.

$$\begin{bmatrix} u^{n+1} \\ v^{n+1} \end{bmatrix} = \begin{bmatrix} u^n \\ v^n \end{bmatrix} - \left(\begin{bmatrix} \frac{\partial Y_1}{\partial u} & \frac{\partial Y_1}{\partial v} \\ \frac{\partial Y_3}{\partial u} & \frac{\partial Y_3}{\partial v} \end{bmatrix}^{-1} \begin{bmatrix} Y_1 \\ Y_3 \end{bmatrix} \right)_{(u^n, v^n)}$$

Now, introduce the following notations,

$$\begin{aligned} \frac{\partial Y_1}{\partial u} &= Y_5, & \frac{\partial Y_2}{\partial u} &= Y_6, & \frac{\partial Y_3}{\partial u} &= Y_7, & \frac{\partial Y_4}{\partial u} &= Y_8, \\ \frac{\partial Y_1}{\partial v} &= Y_9, & \frac{\partial Y_2}{\partial v} &= Y_{10}, & \frac{\partial Y_3}{\partial v} &= Y_{11}, & \frac{\partial Y_4}{\partial v} &= Y_{12}. \end{aligned}$$

As a result of these new notations, the Newton's iterative scheme gets the following form.

$$\begin{bmatrix} u^{n+1} \\ v^{n+1} \end{bmatrix} = \begin{bmatrix} u^n \\ v^n \end{bmatrix} - \left(\begin{bmatrix} Y_5 & Y_9 \\ Y_7 & Y_{11} \end{bmatrix}^{-1} \begin{bmatrix} Y_1 \\ Y_3 \end{bmatrix} \right)_{(u^n, v^n)}$$

Now, differentiating the system of last four first order ODEs with respect to u and v , we get

$$\begin{aligned} Y_5' &= Y_6, & Y_5(0) &= B. \\ Y_6' &= - \left[P_r C_1 Y_6 + \frac{N_c}{Le} (Y_6 Y_4 + Y_2 Y_8) + \frac{2N_c}{Le N_{bt}} Y_2 Y_6 \right], & Y_2(0) &= 1, \\ Y_7' &= Y_8, & Y_7(0) &= 0. \\ Y_8' &= - \left[Sc C_1 Y_8 - \frac{1}{N_{bt}} \left(P_r C_1 Y_6 + \frac{N_c}{Le} (Y_4 Y_6 + y_2 Y_8) + 2 \frac{N_c}{Le N_{bt}} Y_2 Y_6 \right) \right] \\ &\quad - \left[Sc \sigma (1 + \delta^* \theta)^n \exp \left(\frac{-E_1}{1 + \delta^* \theta} \right) Y_7 \right], & Y_8(0) &= 0. \\ Y_9' &= Y_{10}, & Y_9(0) &= 0. \\ Y_{10}' &= - \left[P_r C_1 Y_{10} + \frac{N_c}{Le} Y_4 Y_{10} + Y_2 Y_{12} + 2 \frac{N_c}{Le N_{bt}} Y_2 Y_{10} \right], & Y_{10}(0) &= 0. \\ y_{11}' &= Y_{12}, & Y_{11}(0) &= 0. \\ Y_{12}' &= - \left[Sc C_1 Y_{12} - \frac{1}{N_{bt}} \left(P_r C_1 Y_{10} + \frac{N_c}{Le} (Y_4 Y_{10} + Y_2 Y_{12}) + \frac{2N_c}{Le N_{bt}} Y_2 Y_{10} \right) \right] \\ &\quad - \left[Sc \sigma (1 + \delta^* \theta)^n \exp \left(\frac{-E_1}{1 + \delta^* \theta} \right) Y_{11} \right], & Y_{12}(0) &= 1. \end{aligned}$$

The stopping criteria for the Newton's method is set as

$$\max\{|Y_1(u, v)|, |Y_3(u, v)|\} < \epsilon.$$

4.4 Representation of Graphs and Tables

A detail explanation on the numerical results in the form of the graphs and tables has been discussed. The main focus of this section will be on the influence

of dimensionless parameters on the Skin fraction C_{fx} , Nusselt number Nu_x and Sherwood number Sh_x .

Table (4.1), demonstrate the impact of δ , λ , k_1 and M on the skin friction $Re^{\frac{1}{2}}C_{fx}$. The rising value of above mention parameters the skin fraction $Re^{\frac{1}{2}}C_{fx}$ increases except Williamson parameter λ , by rising Williamson parameter the skin fraction $Re^{\frac{1}{2}}C_{fx}$ decreases.

Table (4.2), shows the impact of the significant parameters like Eckert number, magnetic parameter, Prandtl number, Lewis number, thermophoretic parameter, coefficient of activation energy, temperature ratio parameter and diffusivity ratio parameter on Nusselt number and Sherwood number.

Figures 4.2-4.5, show the effect of distinct parameters on $f'(\eta)$ respectively. By increasing the value of velocity slip parameter δ , the velocity of fluid $f'(\eta)$ decreases as shown in Figures 4.2. The impact of Williamson parameter λ on velocity profile $f'(\eta)$ is shown in Figures 4.3. We observed that the velocity of fluid decreases by increasing the value of Williamson parameter λ . Also by increasing the value of magnetic and porosity parameter the velocity of fluid $f'(\eta)$ decreases as shown in Figures 4.4 and 4.5.

Figures 4.8, 4.9, 4.11, 4.13 and 4.14 demonstrated that by increase the values of the Prandtl number, Lewis number, difusivity ratio parameter, thermal slip parameter and activation energy the temperature profile is declined. While by enhancing the values of Eckert number, magnetic parameter, thermophoretic parameter and temperature ratio parameter the temperature profile $\theta(\eta)$ increases as shown in Figures 4.6, 4.7, 4.10 and 4.12.

The value of concentration profile increases by increasing the values of Prandtl number, magnetic parameter, thermophoretic parameter, temperature ratio parameter and Schmidt number as shown in Figures 4.16, 4.17, 4.18, 4.20 and ?? respectively. While by enhancing the values of Eckert number and activation energy the concentration profile $\phi(\eta)$ decreases as shown in Figures 4.15, and 4.19.

TABLE 4.1: Effects of various parameters on skin fraction

δ	λ	k_1	M	I_m	$C_f x$
0.25	0.5	0.3	0.1	[-0.8,0.8]	-0.98242
0.75				[-0.5,0.8]	-0.59876
1.25				[-0.4,0.8]	-0.44334
1.50				[-0.3,0.8]	-0.39405
0.5				0.1	[-0.5,0.8]
	0.2	[-0.5,0.8]	-0.69913		
	0.8	[-0.5,0.8]	-0.79095		
	1	[-0.6,0.8]	-0.85288		
		0.01	[-0.6,0.8]	-0.66438	
		0.05	[-0.6,0.8]	-0.67514	
		0.1	[-0.5,0.8]	-0.68816	
		0.25	[-0.5,0.8]	-0.72468	
			0	[-0.5,0.8]	-0.71292
			0.05	[-0.5,0.8]	-0.72469
			0.09	[-0.5,0.8]	-0.73782
			0.2	[-0.4,0.8]	-0.75784

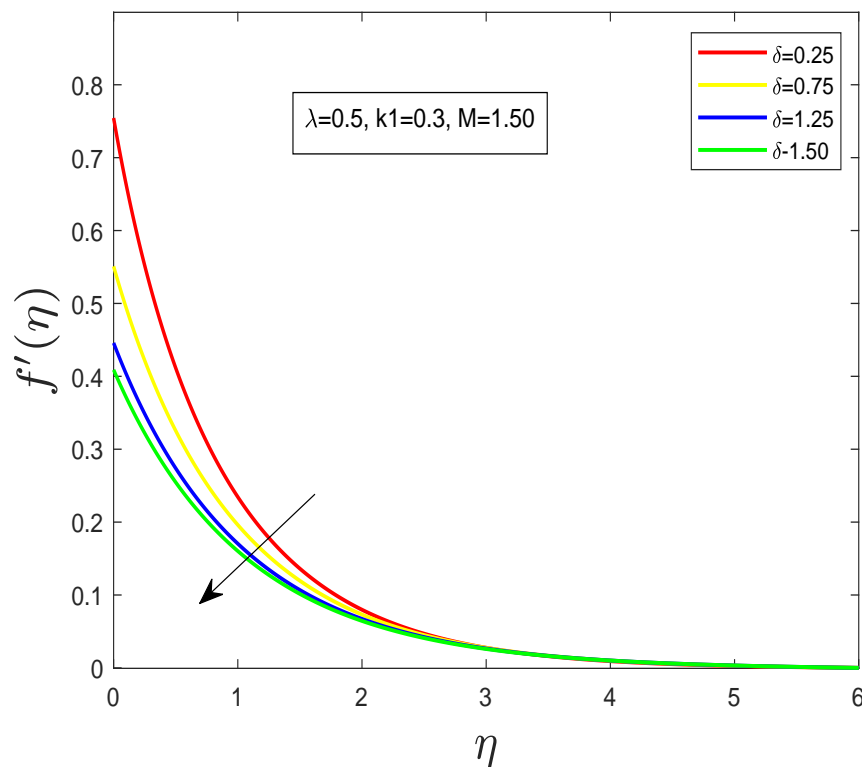
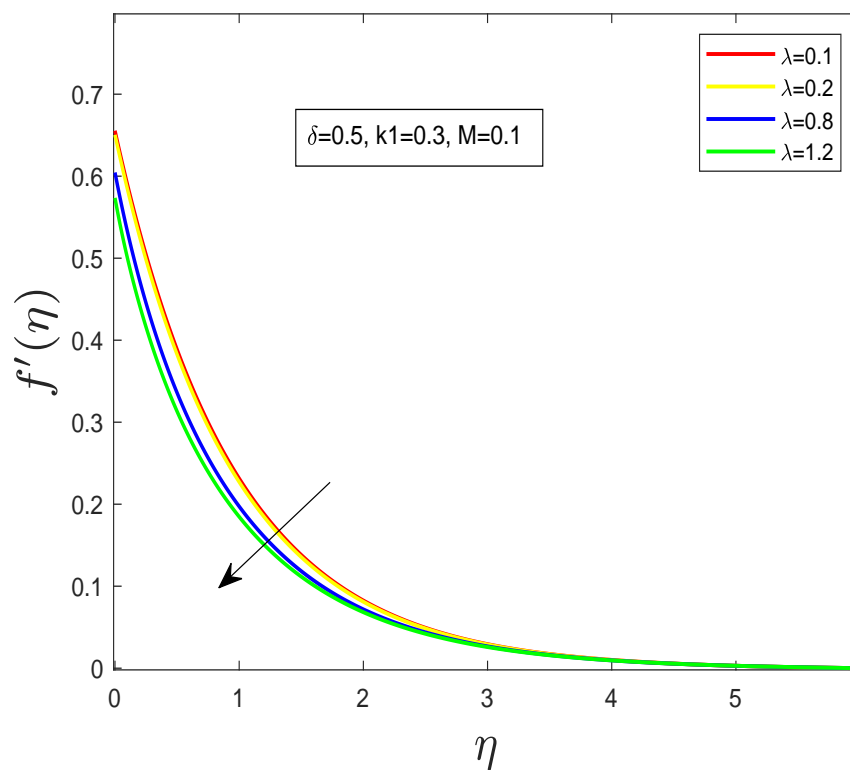
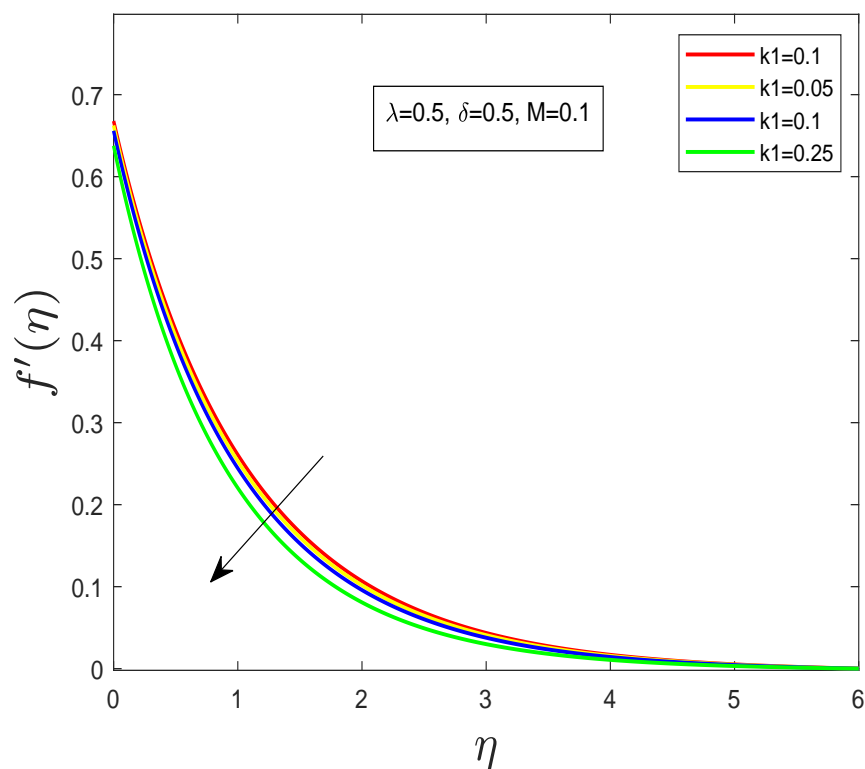


FIGURE 4.2: Change in $f'(\eta)$ for rising value of δ .

TABLE 4.2: Effects of various parameters on Nusselt Number and Sherwood Number

Ec	M	Pr	Le	δ^*	$E1$	σ	I_u	I_v	Nu	Sh
0	0.1	0.5	5	0.1	0.01	0.1	[-0.9,2.0]	[-0.9,0.4]	0.14653	0.98156
0.4							[-0.8,2.0]	[-0.7,0.3]	0.14413	0.98139
0.8							[-0.8,2.0]	[-0.6,0.3]	0.14053	0.98121
1							[-0.7,1.0]	[-0.7,0.3]	0.0.14053	0.98112
0.3	-0.6						[-0.5,0.9]	[-0.5,0.8]	0.19266	1.26103
	-0.2						[-0.4,0.8]	[-0.5,0.8]	0.16038	1.09456
	-0.1						[-0.5,0.9]	[-0.5,0.8]	0.15453	1.05592
	0.1						[-0.5,0.9]	[-0.5,0.8]	0.0.14473	0.98143
		1					[-0.9,0.6]	[-0.9,-0.1]	0.20380	0.91332
		3					[-0.9,0.6]	[-2.0,-0.1]	0.36513	0.99192
		5					[-0.9,0.6]	[-2.0,-0.1]	0.45318	1.03517
		7					[-0.9,0.6]	[-2.0,-0.1]	0.51049	1.06622
			3				[-0.9,4.5]	[-2.0,4.0]	0.15699	0.87425
			7				[-0.9,4.5]	[-0.9,4.0]	0.16536	0.87907
			10				[-0.8,0.8]	[-0.8,0.8]	0.17677	0.88571
			12				[-0.8,0.8]	[-0.8,0.8]	0.18760	0.89170
				-0.5			[-0.9,0.8]	[-2.0,-0.1]	0.14771	1.17252
				0			[-0.8,0.7]	[-2.0,-0.2]	0.14533	0.97795
				0.2			[-0.7,0.6]	[-2.0,-0.3]	0.14640	0.70484
				0.4			[-0.7,0.6]	[-2.0,-0.3]	0.14744	0.45619
					0.5		[-0.9,0.9]	[-3,-0.1]	0.14539	0.99147
					2.5		[-0.8,0.9]	[-3,-0.1]	0.14489	1.15690
					5		[-0.9,0.9]	[-3,-0.1]	0.14481	1.18303
					7		[-0.9,0.9]	[-3,-0.1]	0.14480	1.18546
						-0.03	[-0.9,0.9]	[-3,-0.1]	0.14456	1.26991
						0	[-0.9,0.9]	[-3,-0.1]	0.14481	1.18587
						0.01	[-0.9,0.9]	[-3,-0.1]	0.14489	1.15684
						0.06	[-0.9,0.9]	[-3,-0.1]	0.14536	1.00298

FIGURE 4.3: Effect of Williamson parameter λ on velocity profile $f'(\eta)$.FIGURE 4.4: Effect of porosity k_1 on velocity profile $f'(\eta)$.

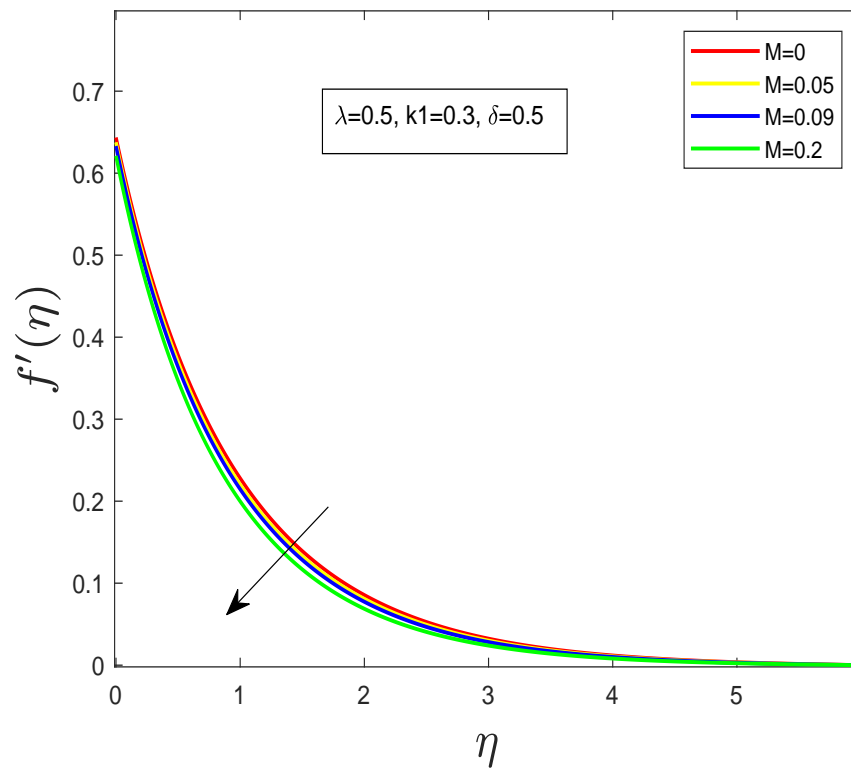


FIGURE 4.5: Effect of Magnetic parameter M on velocity profile $f'(\eta)$.

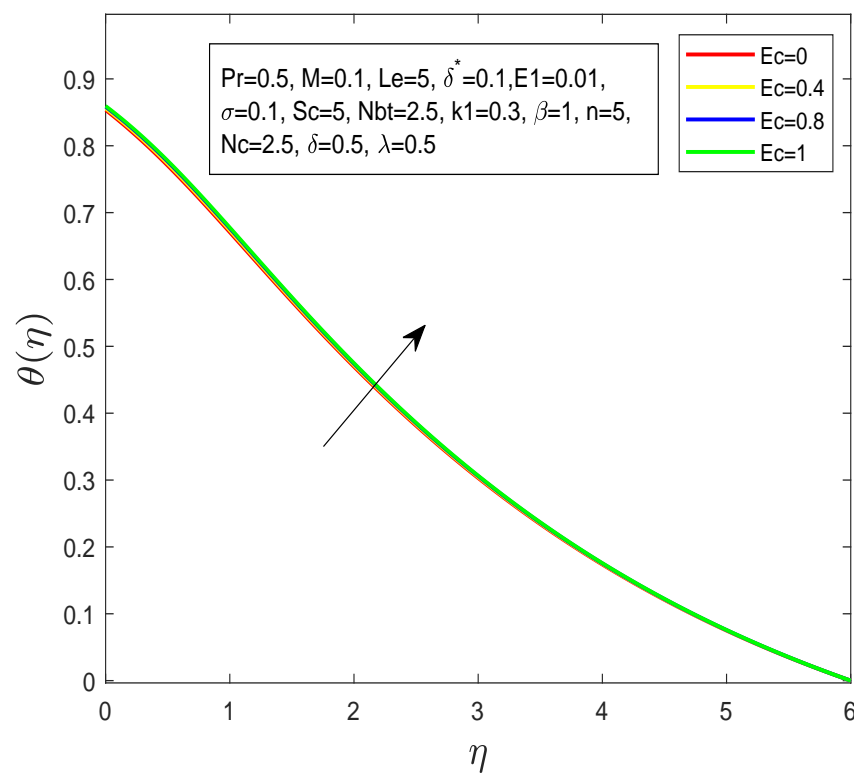
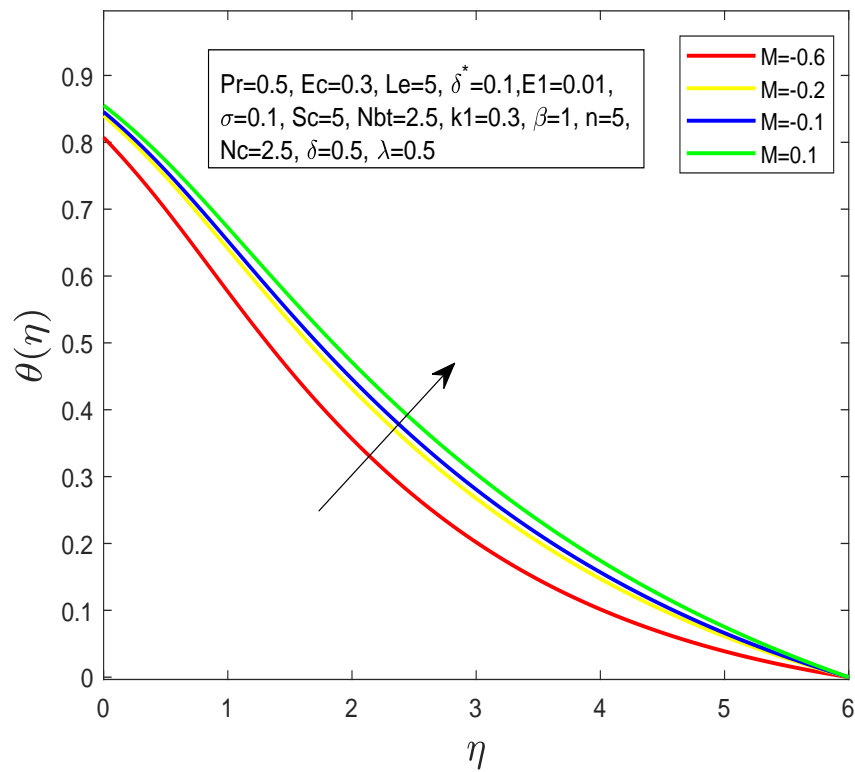
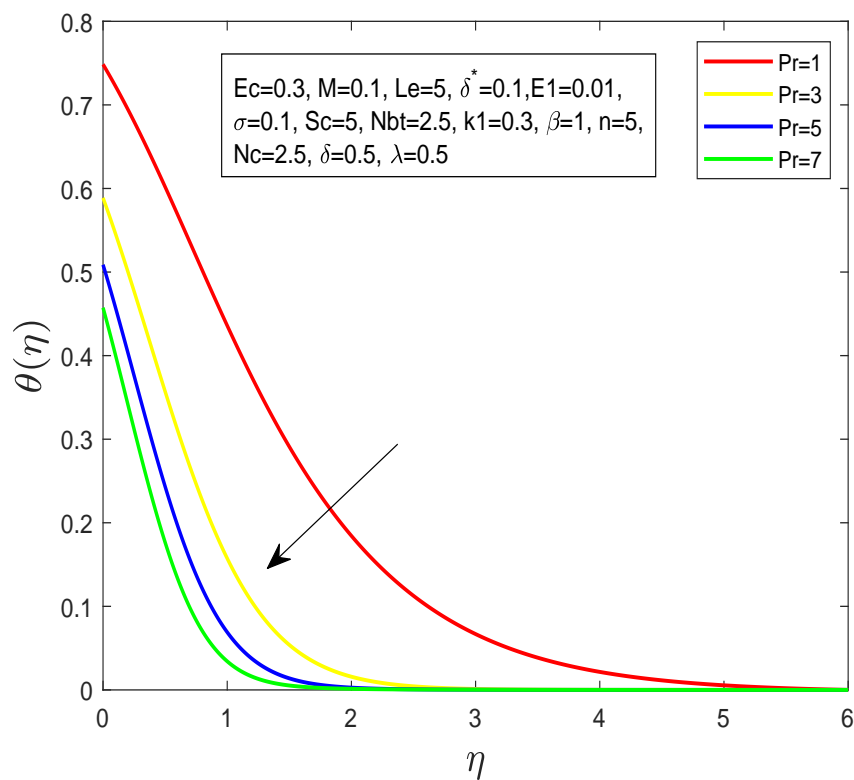


FIGURE 4.6: Effect of Eckert number E_c on temperature profile $\theta(\eta)$.

FIGURE 4.7: Effect of magnetic parameter M on temperature profile $\theta(\eta)$.FIGURE 4.8: Effect of Prandtl number Pr on temperature profile $\theta(\eta)$.

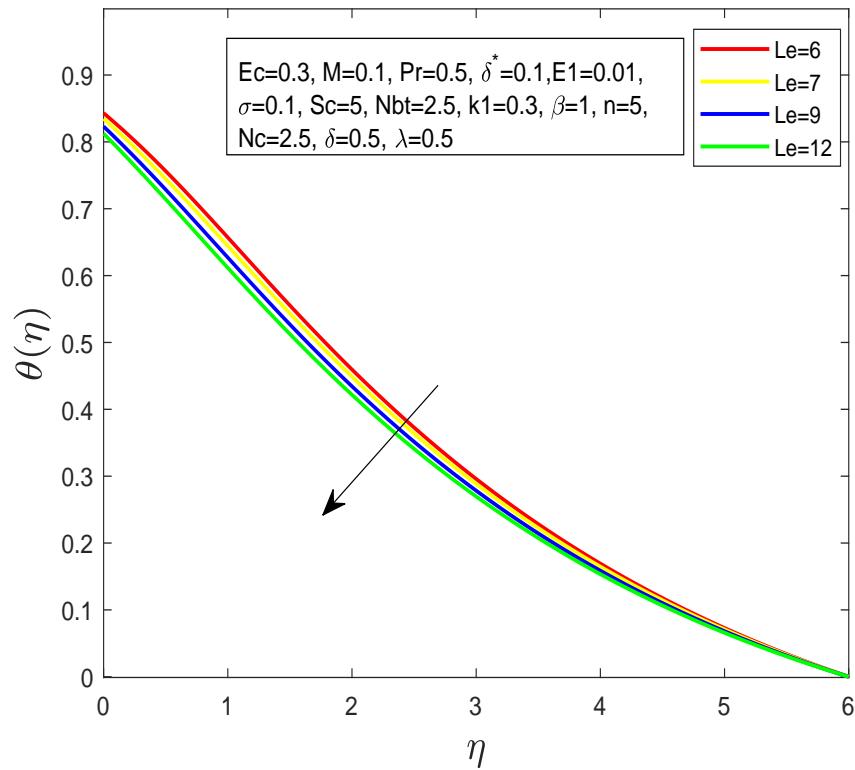


FIGURE 4.9: Effect of Lewis number on temperature profile $\theta(\eta)$.

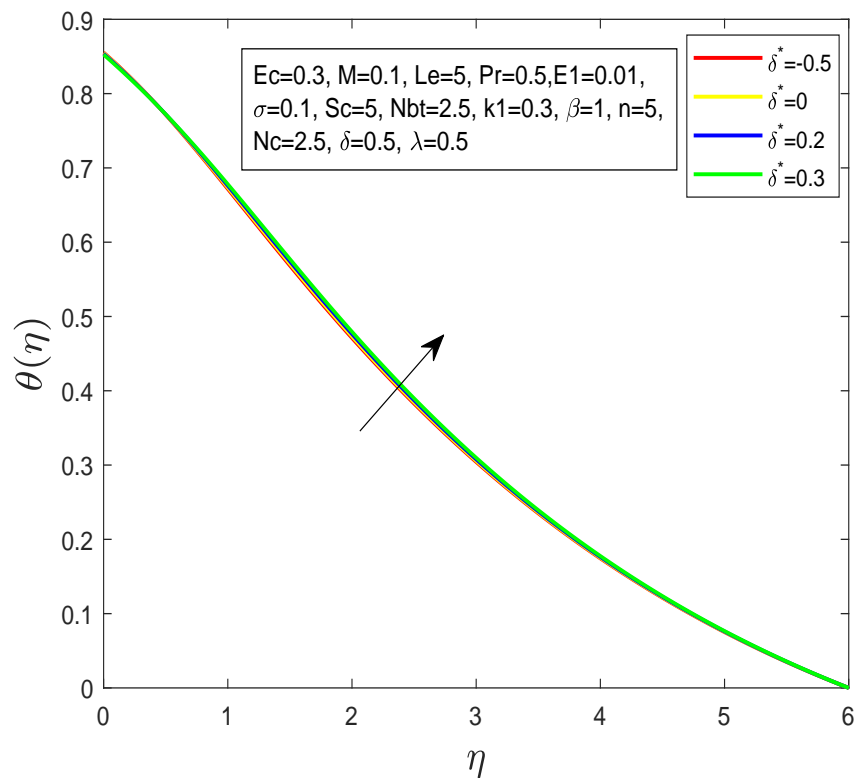


FIGURE 4.10: Effect of Thermophoretic parameter δ^* on temperature profile.

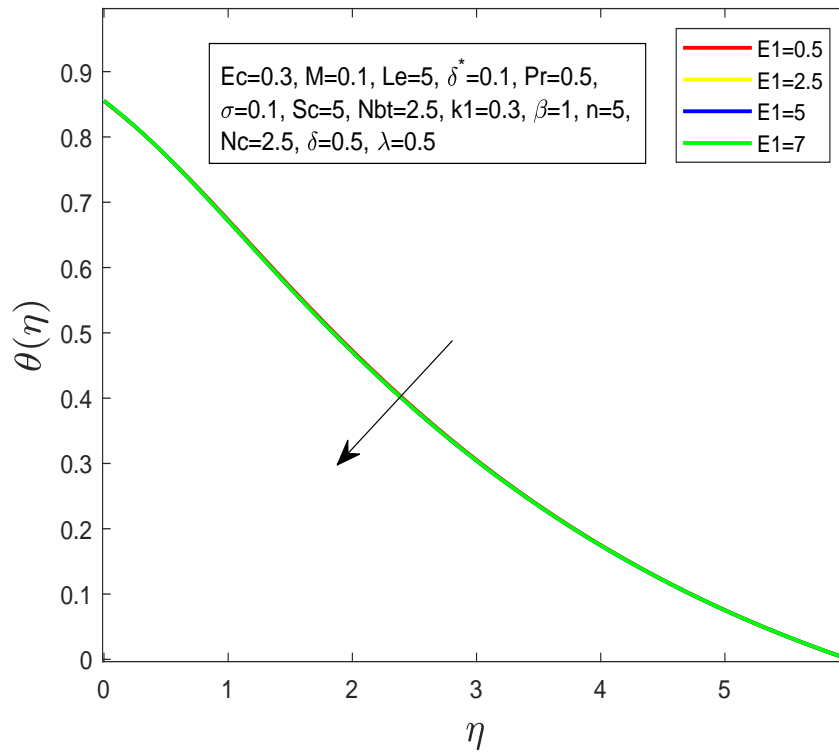


FIGURE 4.11: Effect of coefficient of activation energy $E1$ on temperature profile $\theta(\eta)$.

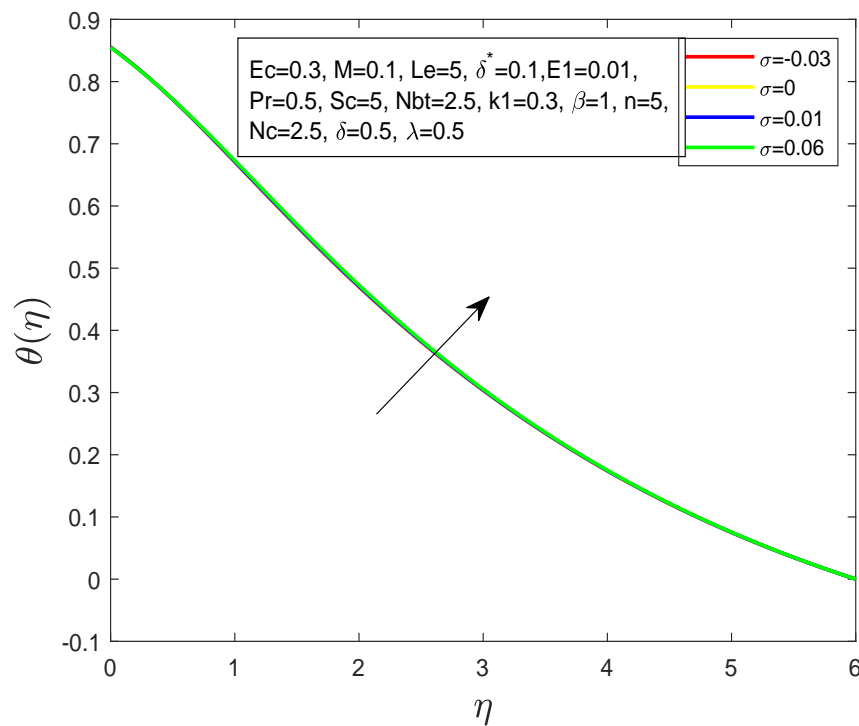


FIGURE 4.12: Effect of temperature ratio parameter σ on temperature profile $\theta(\eta)$.

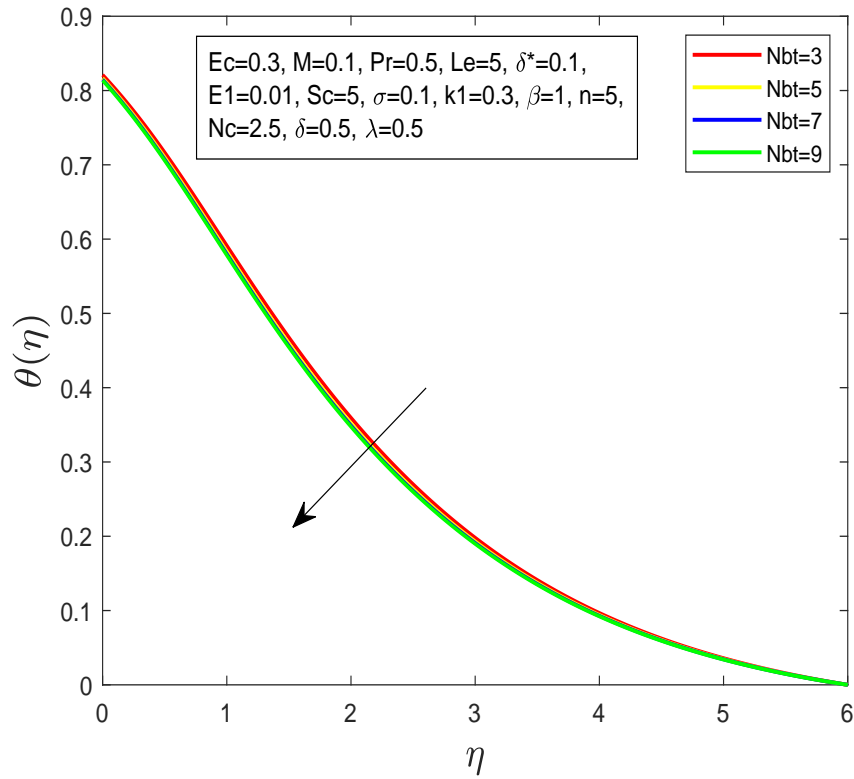


FIGURE 4.13: Effect of diffusivity ratio parameter Nbt on temperature profile $\theta(\eta)$.

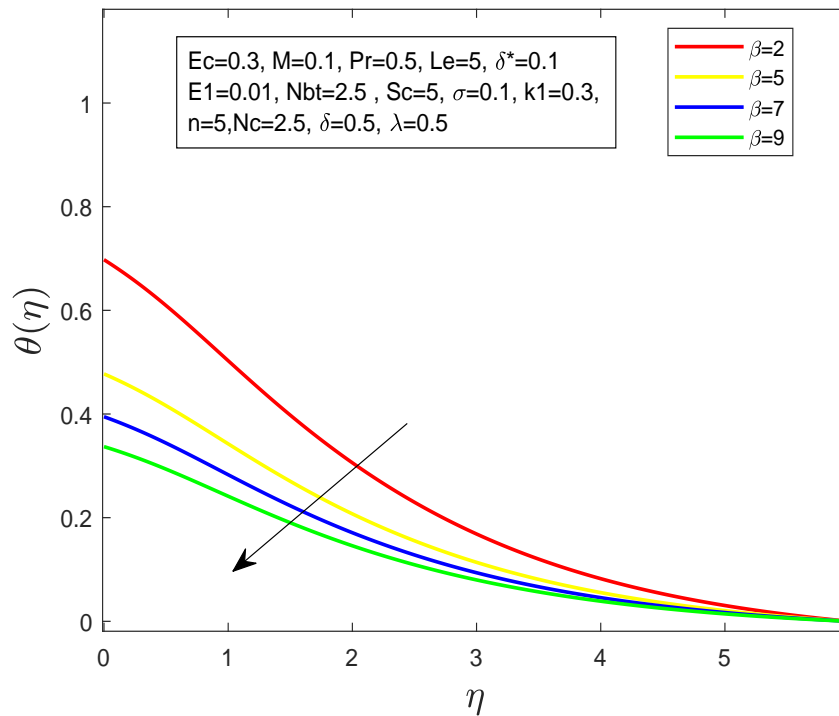


FIGURE 4.14: Effect of thermal slip parameter β on temperature profile $\theta(\eta)$.

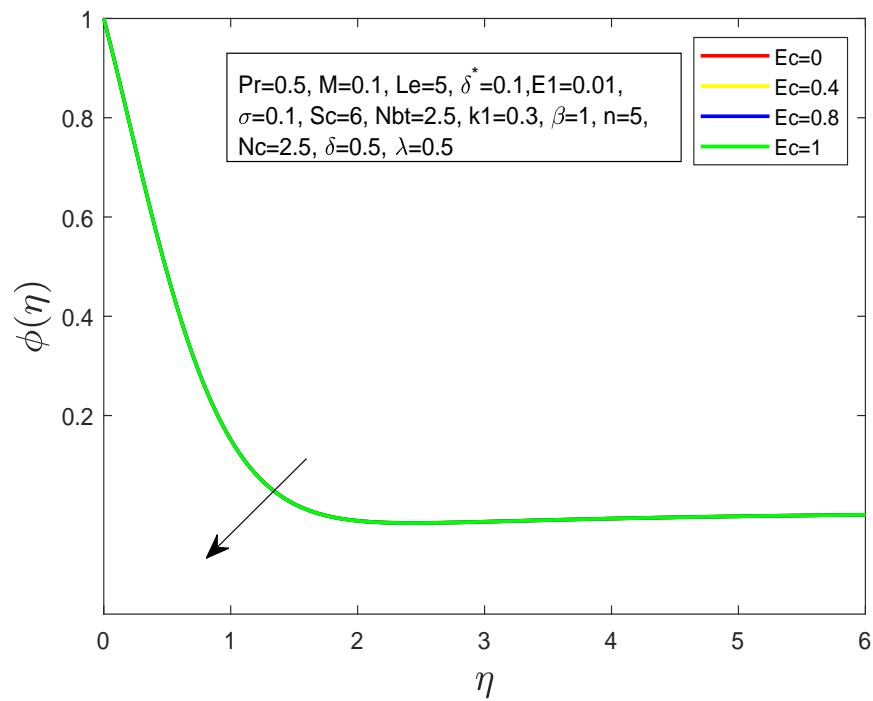


FIGURE 4.15: Effect of Eckert number Ec on concentration profile $\phi(\eta)$.

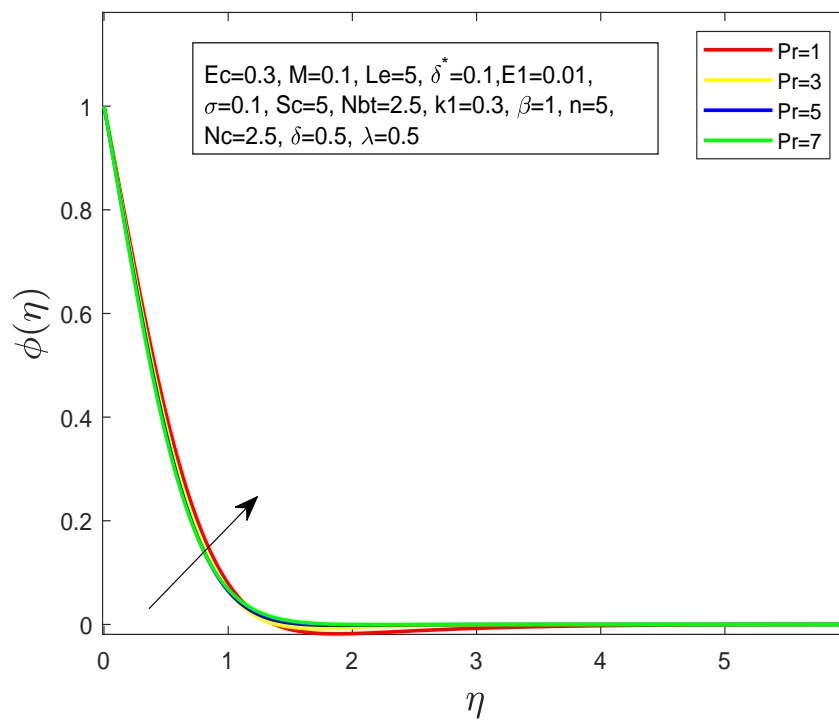


FIGURE 4.16: Effect of Prandtl number Pr on concentration profile $\phi(\eta)$.

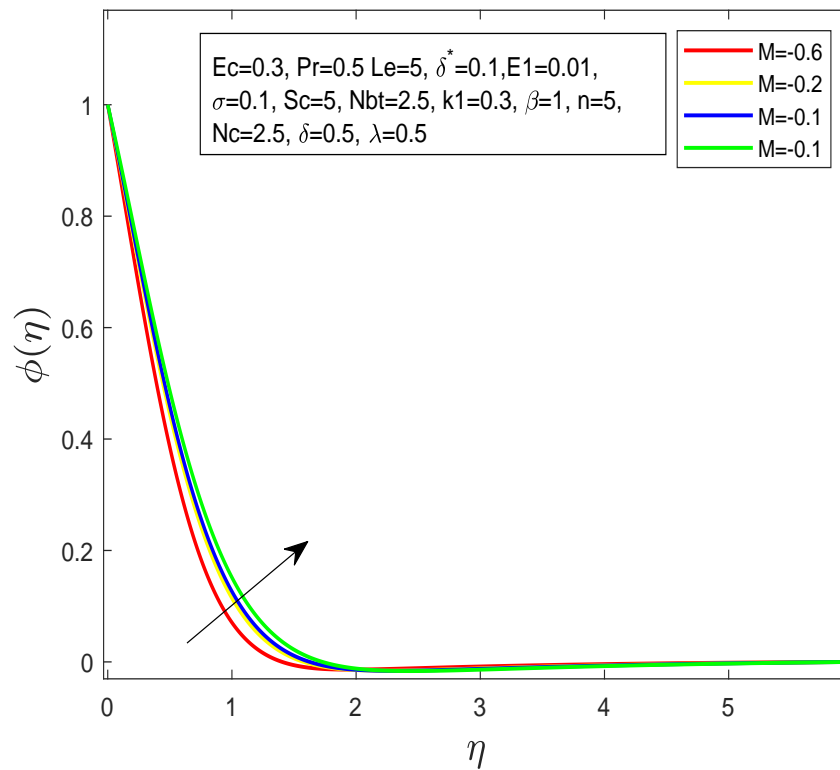


FIGURE 4.17: Effect of Magnetic parameter M on concentration profile $\phi(\eta)$.

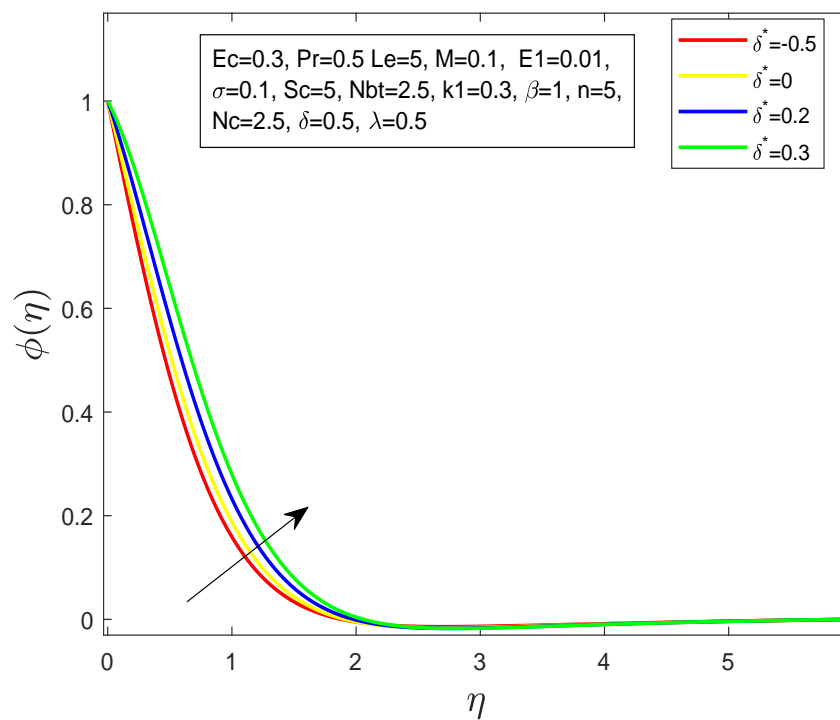


FIGURE 4.18: Effect of thermophoretic parameter δ^* on concentration profile $\phi(\eta)$.

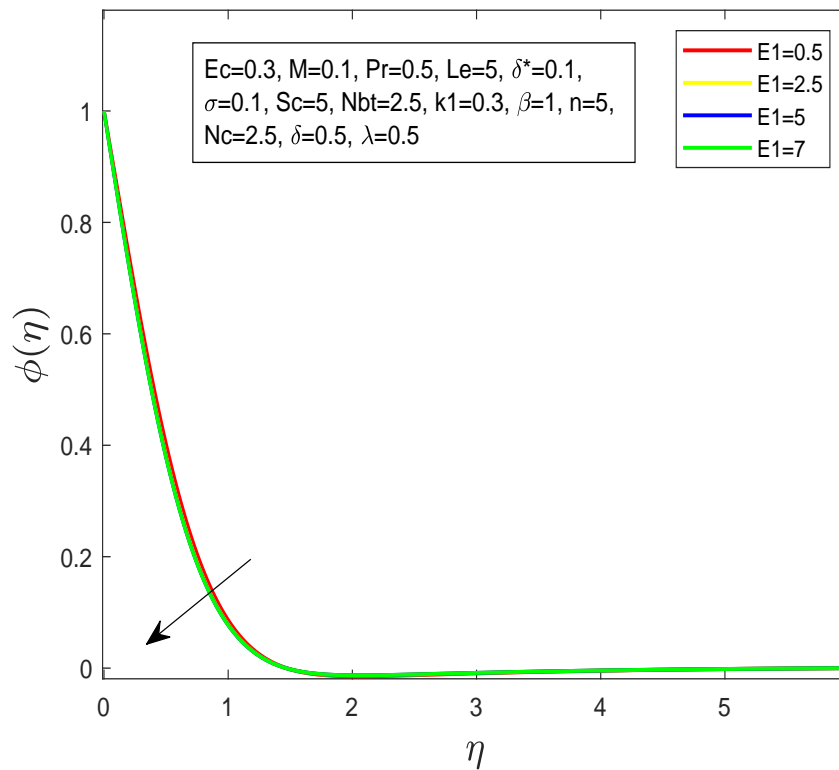


FIGURE 4.19: Effect of coefficient of activation energy $E1$ on concentration profile $\phi(\eta)$.

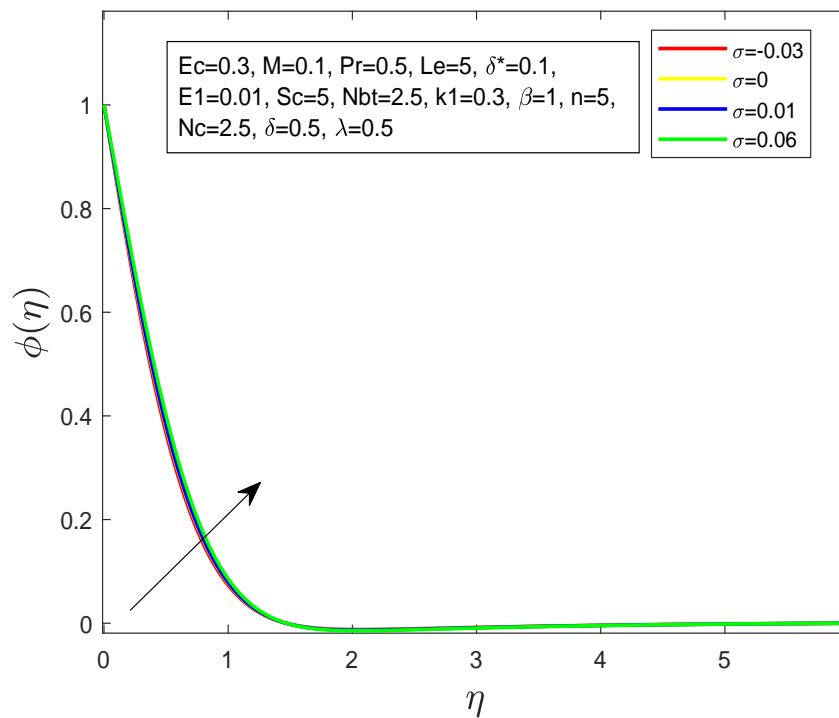


FIGURE 4.20: Effect of temperature ratio parameter σ on concentration profile $\phi(\eta)$.

Chapter 5

Conclusion

In this research work, the work of Y. B. Kho et al. [32] is reviewed and extended by the addition of MHD, porous parameter, activation energy and Joule heating. By using similarity transformations, the momentum equation, heat equation and concentration equation are converted into ODEs. Furthermore, the numerical solution of these converted ODEs has been analyzed by using shooting technique. Considering different parameters and using different values of these parameters, the results are presented in the form of tables and graphs for velocity, temperature and concentration profile. The important results of current research can be precise as below.

- By increasing the value of the velocity slip δ and Williamson parameter λ , the values of the velocity profile increase while temperature profile is decreased.
- As we increase the value of Prandtl number Pr , Lewis number Le , diffusivity ratio parameter Nbt and thermal slip parameter β , the the value of temperature profile is declined.
- The concentration profile decreases by increasing the values of Schmidt number Sc , diffusivity ratio parameter Nbt and thermal slip parameter β , while the concentration profile is increased by increasing the values of the velocity slip parameter δ and the Williamson parameter λ .

-
- For rising the value of the velocity slip parameter δ , the skin friction coefficient is increased. However by increasing the value of Williamson parameter λ , the skin friction coefficient is dropped.
 - It is found that values of Nusselt number and Sherwood number fall down by increasing the values of δ and λ , while an ascending pattern of Nusselt and Sherwood is found for increasing values of Pr , Sc and Le .
 - A decrement is noticed in the temperature profile due to ascending values of the Eckert number Ec .
 - Due to the decreasing values of M and k_1 , the velocity profile is increased.

Bibliography

- [1] J. Buongiorno, “Convective transport in nanofluids.” ASME.J. Heat transfer,” March 2006.
- [2] M. Corcione, M. Cianfrini, and A. Quintino, “Two-phase mixture modeling of natural convection of nanofluids with temperature-dependent properties,” *International Journal of Thermal Sciences*, vol. 71, pp. 182–195, 2013.
- [3] F. Garoosi, S. Garoosi, and K. Hooman, “Numerical simulation of natural convection and mixed convection of the nanofluid in a square cavity using Buongiorno’s model,” *Powder Technology*, vol. 268, pp. 279–292, 2014.
- [4] S. Eiamsa-Ard, K. Kiatkittipong, and W. Jedsadaratanachai, “Heat transfer enhancement of TiO_2 -water nanofluid in a heat exchanger tube equipped with overlapped dual twisted-tapes,” *Engineering Science and Technology. An International Journal*, vol. 18, no. 3, pp. 336–350, 2015.
- [5] M. Turkyilmazoglu, “Exact analytical solutions for heat and mass transfer of mhd slip flow in nanofluids,” *Chemical Engineering Science*, vol. 84, pp. 182–187, 2012.
- [6] M. Qasim, Z. Khan, R. Lopez, and W. Khan, “Heat and mass transfer in nanofluid thin film over an unsteady stretching sheet using Buongiorno’s model,” *The European Physical Journal Plus*, vol. 131, no. 1, pp. 1–11, 2016.
- [7] A. Hussanan, M. Z. Salleh, and I. Khan, “Microstructure and inertial characteristics of a magnetite ferrofluid over a stretching/shrinking sheet using effective thermal conductivity model,” *Journal of Molecular Liquids*, vol. 255, pp. 64–75, 2018.

- [8] “Heat transfer flow of Cu-water and Al₂O₃-water micropolar nanofluids about a solid sphere in the presence of natural convection using Keller-box method, author=Swalmeh, Mohammed Z and Alkasasbeh, Hamzeh T and Hussanan, Abid and Mamat, Mustafa,” *Results in Physics*, vol. 9, pp. 717–724, 2018.
- [9] M. I. Afridi, M. Qasim, and S. Saleem, “Second law analysis of three dimensional dissipative flow of hybrid nanofluid,” *Journal of Nanofluids*, vol. 7, no. 6, pp. 1272–1280, 2018.
- [10] M. Krishnamurthy, B. Gireesha, B. Prasannakumara, and R. S. R. Gorla, “Thermal radiation and chemical reaction effects on boundary layer slip flow and melting heat transfer of nanofluid induced by a nonlinear stretching sheet,” *Nonlinear Engineering*, vol. 5, no. 3, pp. 147–159, 2016.
- [11] H. Blasius, “The boundary layers in fluids with little friction,” 1950.
- [12] “Boundary-layer behavior on continuous solid surfaces. I:Boundary-layer equations for two-dimensional and axisymmetric flow.”
- [13] G. Ramesh, B. Gireesha, and R. S. R. Gorla, “Study on Sakiadis and Blasius flows of Williamson fluid with convective boundary condition,” *Nonlinear Engineering*, vol. 4, no. 4, pp. 215–221, 2015.
- [14] N. A. Khan and H. Khan, “A Boundary layer flow of non-Newtonian Williamson fluid,” *Nonlinear Engineering*, vol. 3, no. 2, pp. 107–115, 2014.
- [15] S. Nadeem and S. Hussain, “Analysis of MHD Williamson Nano Fluid Flow over a Heated Surface.” *Journal of Applied Fluid Mechanics*, vol. 9, no. 2, pp. 729–739, 2016.
- [16] C. Kurtcebe and M. Erim, “Heat transfer of a non-Newtonian viscoelastic fluid in an axisymmetric channel with a porous wall for turbine cooling application,” *int. commun. Heat Transfer*, vol. 29, no. 7, pp. 971–982, 2002.

- [17] “MHD boundary layer flow and heat transfer of a nanofluid past a permeable stretching sheet with velocity, thermal and solutal slip boundary conditions, author=Ibrahim, Wubshet and Shankar, Bandari,” *Computers & Fluids*, vol. 75, pp. 1–10, 2013.
- [18] M. Krishnamurthy, B. Prasannakumara, B. Gireesha, and R. S. R. Gorla, “Effect of chemical reaction on MHD boundary layer flow and melting heat transfer of Williamson nanofluid in porous medium,” *Engineering Science and Technology; an International Journal*, vol. 19, no. 1, pp. 53–61, 2016.
- [19] Y. Xuan and Q. Li, “Investigation on convective heat transfer and flow features of nanofluids,” *journal of Heat transfer*, vol. 125, no. 1, pp. 151–155, 2003.
- [20] S. Z. Heris, S. G. Etemad, and M. N. Esfahany, “Experimental investigation of oxide nanofluids laminar flow convective heat transfer,” *International Communications in Heat and Mass Transfer*, vol. 33, no. 4, pp. 529–535, 2006.
- [21] F. Yang, “Slip boundary condition for viscous flow over solid surfaces,” *Chemical Engineering Communications*, vol. 197, no. 4, pp. 544–550, 2009.
- [22] A. Noghrehabadi, R. Pourrajab, and M. Ghalambaz, “Effect of partial slip boundary condition on the flow and heat transfer of nanofluids past stretching sheet prescribed constant wall temperature,” *International Journal of Thermal Sciences*, vol. 54, pp. 253–261, 2012.
- [23] A. Malvandi, F. Hedayati, and D. Ganji, “Slip effects on unsteady stagnation point flow of a nanofluid over a stretching sheet,” *Powder Technology*, vol. 253, pp. 377–384, 2014.
- [24] A. Raisi, B. Ghasemi, and S. Aminossadati, “A numerical study on the forced convection of laminar nanofluid in a microchannel with both slip and no-slip conditions,” *Numerical Heat Transfer, Part A: Applications*, vol. 59, no. 2, pp. 114–129, 2011.

-
- [25] R. W. Fox, A. McDonald, and P. Pitchard, *Introduction to Fluid Mechanics*. John Wiley & Sons, Inc, 2006.
- [26] Y. A. Cengel, *Fluid mechanics*. Tata McGraw-Hill Education, 2010.
- [27] R. Bansal, *A Textbook of Fluid Mechanics and Hydraulic Machines*. Laxmi publications, 2004.
- [28] Modi and Seth, *Fluid Mechanic*. Standard Book House, 2011.
- [29] Davidson, *An Introduction to Magnetohydrodynamics (Cambridge Texts in Applied Mathematics)*. Cambridge University Press. doi:10.1017/CBO9780511626333, 2001.
- [30] T. Hassan and M. Anwar, *Physics*. Carvan Book House, 2010.
- [31] J. Ahmed and M. S. Rahman, *Handbook of Food Process Design*. John Wiley & Sons, 2012.
- [32] Y. B. Kho, A. Hussanan, M. K. A. Mohamed, and M. Z. Salleh, “Heat and mass transfer analysis on flow of Williamson nanofluid with thermal and velocity slips: Buongiorno model,” *Propulsion and Power Research*, vol. 8, no. 3, pp. 243–252, 2019.
- [33] M. Gad-el Hak, *Frontiers in Experimental Fluid Mechanics*. Springer Science & Business Media, 2013, vol. 46.
- [34] R. W. Lewis, P. Nithiarasu, and K. N. Seetharamu, *Fundamentals of the Finite Element Method for Heat and Fluid Flow*. John Wiley & Sons, 2004.
- [35] J. Kunes, *Dimensionless physical quantities in science and engineering*. Laxmi publishers, 2004.
- [36] J. N. Reddy and D. K. Gartling, *The Finite Element Method in Heat Transfer and Fluid Dynamics*. CRC press, 2010.